Tectonics

RESEARCH ARTICLE
10.1029/2019TC005780

Special Section:
Tectonic evolution of West-Central Tethysides

Lower Cretaceous Provenance and Sedimentary Deposition in the Eastern Carpathians: Inferences for the Evolution of the Subducted Oceanic Domain and its European Passive Continental Margin

R. D. Roban[1], M. N. Ducea[2,1], L. Mațenco[3], G. C. Panaiotu[4], L. Profeta[1,2], C. Krézsek[5], M. C. Melinte-Dobrinescu[6], N. Anastasiu[1], D. Dimofte[1], V. Apotrosoaei[1], and I. Francovschi[1]

[1]Faculty of Geology and Geophysics, University of Bucharest, Bucharest, Romania, [2]Department of Geosciences, University of Arizona, Tucson, AZ, USA, [3]Faculty of Geosciences, Utrecht University, Utrecht, Netherlands, [4]Faculty of Physics, University of Bucharest, Bucharest, Romania, [5]OMV Petrom, Bucharest, Romania, [6]National Institute of Marine Geology and Geo-Ecology, Bucharest, Romania

Abstract Reconstructing orogenic systems made up dominantly by sediments accreted in trenches is challenging because of the incomplete lithological record of the subducted oceanic domain and its attached passive continental margin thrusted by collisional processes. In this respect, the remarkable ~600 km long continuity of sediments exposed in the Eastern Carpathian thin-skinned thrust and fold belt and the availability of quantitative reconstructions for adjacent continental units provide excellent conditions for a paleogeographical study by provenance and sedimentological techniques constraining sediment routing and depositional systems. These sediments were deposited in the Ceahlău-Severin branch of the Alpine Tethys Ocean and over its European passive continental margin. We report sedimentological, paleomagnetic, petrographic, and detrital zircon U-Pb data of Lower Cretaceous sediments from several thin-skinned tectonic units presumably deposited in the Moldavides domain of the Eastern Carpathians. Sedimentological observations in the innermost studied unit demonstrate that deposition took place in a deepwater basin floor sheets to sandy turbidite system. Detrital zircon age data demonstrate sourcing from internal Carpathian basement units. The sediment routing changes in more external units, where black shales basin floor sheets to sandy mud turbidites were sourced from an external, European continental area. Although some degree of mixing between sources located on both margins of the ocean occurred, constraining a relatively narrow width of the deep oceanic basin, these results demonstrate that the internal-most studied unit was deposited near an Early Cretaceous accretionary wedge, located on the opposite internal side relative to the passive continental margin domain of other Moldavides units.

Key Points:
- Quantitative reconstruction of sediment routing constrained the paleogeography in the key studied areas of the Eastern Carpathians
- The Lower Cretaceous basin accommodated pelagic and turbidite sediments supplied by its both active and passive continental margins
- The partial closure of the ocean activated internal source areas along the continental margin of the Dacia tectonic mega-unit

Supporting Information:
- Supporting Information S1
- Table S1
- Table S2
- Data Set S1

Correspondence to:
R. D. Roban and M. C. Melinte-Dobrinescu,
reludumitru.roban@g.unibuc.ro;
melinte@geoecomar.ro

Citation:
Roban, R. D., Ducea, M. N., Mațenco, L., Panaiotu, G. C., Profeta, L., Krézsek, C., et al. (2020). Lower Cretaceous provenance and sedimentary deposition in the Eastern Carpathians: Inferences for the evolution of the subducted oceanic domain and its European passive continental margin. *Tectonics*, *39*, e2019TC005780. https://doi.org/10.1029/2019TC005780

Received 22 JUL 2019
Accepted 14 APR 2020
Accepted article online 20 APR 2020

1. Introduction

Quantitative paleogeographic reconstructions of orogenic domains are challenging because of the large amounts of oceanic and continental materials lost by subduction processes, which are only partly recycled in magmatic arcs or accreted during convergence (e.g., DeCelles et al., 2009; Handy et al., 2010; Menant et al., 2016). The situation is even more challenging when the orogenic system contains mostly sediments accreted in trenches, with little to no direct record of the geometry and composition of the subducted lithosphere of the ocean and its attached passive continental margin thrusted by collisional processes (e.g., Marshak, 1988; Pfiffner, 2006; Roure, 2008). In such situations, one optimal technique to quantify depositional environments and sediment routing is integrated provenance and sedimentological studies in thin-skinned thrust belts that take advantage of advanced geochronological techniques (e.g., Bush et al., 2016; Pastor-Galán et al., 2013; Pecha et al., 2018). The power of such techniques is enhanced by the availability of regional quantitative reconstructions, where the evolution of large continental units is more precisely derived from the higher resolution record of continental breakup and oceanic drifting available in surrounding areas (e.g., Gaina et al., 2013; Torsvik et al., 2010; van Hinsbergen et al., 2020).

10.1029/2019TC005780

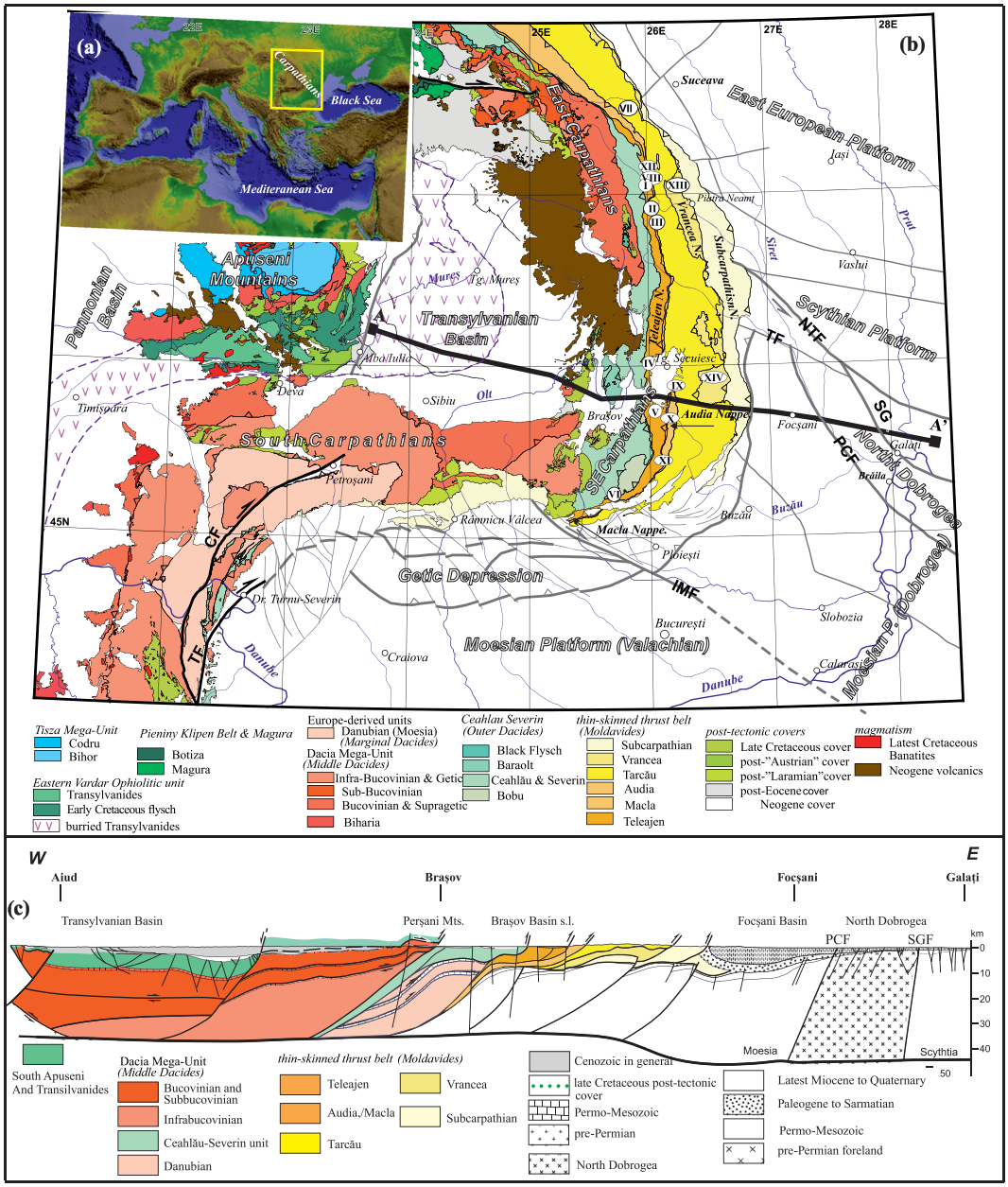

Figure 1. (a) Location of the Carpathians in the European system of mountain ranges. The inset is the location of Figure 1b; (b) Tectonic map of the Romanian Carpathians (after Mațenco, 2017 and references therein). I to XIV are the locations of the samples and outcrops described on this study; NTF - North Trotuș Fault, TF - Trotuș Fault, PCF - Peceneaga-Camena Fault, SG - Sfântu Gheorge Fault; IMF - Intra-Moesian Fault, CF - Cerna Fault, TF - Timok Fault. A–A′ is the location of the cross-section in Figure 1c. (c) NW to SE cross section across the Transylvanian Basin, Southeastern Carpathians and their European foreland (slightly modified from Schmid et al., 2008).

One interesting place to understand the geometry of the subducted ocean and its attached passive continental margin is the Carpathians system of Central Europe (Figure 1a). The Carpathians and their transition into the Balkanides Mountains represent a highly curved orogenic system that formed in response to the opening and closure of an oceanic domain that was kinematically linked to the Alpine Tethys Ocean (e.g., Favre & Stampfli, 1992; Plašienka, 2018; Schmid et al., 2008). Building on numerous previous studies, the Jurassic to Miocene evolution of surrounding continental units has been more precisely and quantitatively reconstructed by accounting for the record of continental breakup,

drifting, subduction, and collision in the larger Mediterrean domain (van Hinsbergen et al., 2020, and references therein). We know that the Middle to Late Jurassic opening of the Ceahlău-Severin branch of the Alpine Tethys Ocean in the Romanian segment of the Carpathians was followed by its closure, when orogenic deformation peaked during two late Early and latest Cretaceous events and was followed by an Oligocene-Miocene period of prolonged collision (e.g., Csontos & Vörös, 2004; Mațenco, 2017; Săndulescu, 1988, 1994; Schmid et al., 2008). In terms of paleogeography, sediments presently exposed in the Ceahlău and Severin nappes of the Eastern and Southern Carpathians, respectively, were deposited in a domain (the External Dacides of Săndulescu, 1984) characterized by oceanic basement (and hence the name of the ocean), whose mafic remnants are scarcely exposed in these nappes. However, despite numerous sedimentological and tectonic studies (e.g., Olariu et al., 2014; Roban et al., 2017; Schmid et al., 2020, and references therein), the routing and nature of the basement underlying the Lower Cretaceous sediments observed in more external Moldavides nappes (sensu Săndulescu, 1984), in terms of oceanic or (hyper)extended continental lithosphere, is still not understood (e.g., Mațenco, 2017, and references therein). This lack of understanding owes to the poor knowledge of the extent of the later subducted European-derived passive continental margin, which likely followed roughly the present-day curved geometry of the Carpathians contact with their foreland platform units (Figure 1b) (e.g., Schmid et al., 2008; Tari, 2005; Ustaszewski et al., 2008). Understanding the paleogeography of this passive continental margin has wide ranging implications, from subduction mechanics to the oceanic to continental mantle nature of the Vrancea subducted slab, presently observed by teleseismic tomography studies beneath the south-eastern Carpathians (for geometry and details, see, for instance, Balázs et al., 2017; Bokelmann & Rodler, 2014; Martin & Wenzel, 2006).

Previous studies showed that the Severin part of the oceanic lithosphere was already subducted in the Southern Carpathians segment by late Early Cretaceous times (~110 – 100 Ma) (e.g., Schmid et al., 2008, and references therein). Coeval thrusting occurred in the Bucovinian and Getic basement nappe system of the Eastern and Southern Carpathians, respectively, which formed the upper plate continental margin in respect to the subduction of the Ceahlău-Severin oceanic basin (Figures 1b and 1c) (e.g., Iancu et al., 2005a; Kräutner & Bindea, 2002; Săndulescu, 1994). These nappes contain basement rocks that were previously part of a system of Neoproterozoic to Paleozoic peri-Gondwanan arc and back-arc terranes, which were metamorphosed during Paleozoic times (Figures 1b and 1c) (e.g. Balintoni et al., 2011a; Balintoni et al., 2014; Ducea et al., 2016; Iancu, Berza, Seghedi, Gheuca, & Hann, 2005a; Iancu et al., 2005b). On the other continental margin of the former Ceahlău-Severin Ocean, provenance studies have shown that the units of the stable European foreland contain essentially Late Proterozoic basement ages and are derived from both European and Gondwana margins, most probably amalgamated by the end of Paleozoic times (the East European, Moesian, and Scythian platforms; Figures 1b and 1c) (e.g., Săndulescu & Visarion, 1988; Seghedi et al., 2005; Vaida et al., 2005; Visarion et al., 1988).

The different early and inherited evolution of the continental basement units located on both sides of the Ceahlău-Severin Ocean open up the possibility of combining sedimentological and geochronological studies to establish the provenance of sediments deposited in the oceanic basin and its European continental passive margin. By taking advantage of the remarkable continuity of stratigraphy along 600 km orogenic strike of the Eastern Carpathians, we performed a study of the Valanginian-Albian black shales and sand-prone succession in a number of key locations of the Moldavides nappe system that are correlated by extensive descriptions available in previous studies (e.g., Contescu, 1974; Melinte-Dobrinescu & Roban, 2011; Roban et al., 2017; Roban & Melinte-Dobrinescu, 2012) (see supporting information, Figure S1). Furthermore, we analyze the balance between sourcing from the two margins of the ocean and intrabasinal source areas inferred to have been inherited from the pre-orogenic evolution of the European passive continental margin (the platform ridges of Filipescu & Alexandrescu, 1962; Grigorescu & Anastasiu, 1976; Murgeanu, 1937). Our main approach is a combination between a depositional model that uses the principles of facies analysis based on outcrop studies and petrographic and detrital zircon (DZ) U-Pb data. These investigations allow constraining the source areas during the Lower Cretaceous deposition. Additionally, these data are combined with available plate tectonic reconstructions to infer the geometry and extent of the Ceahlău-Severin Ocean and its former European passive continental margin.

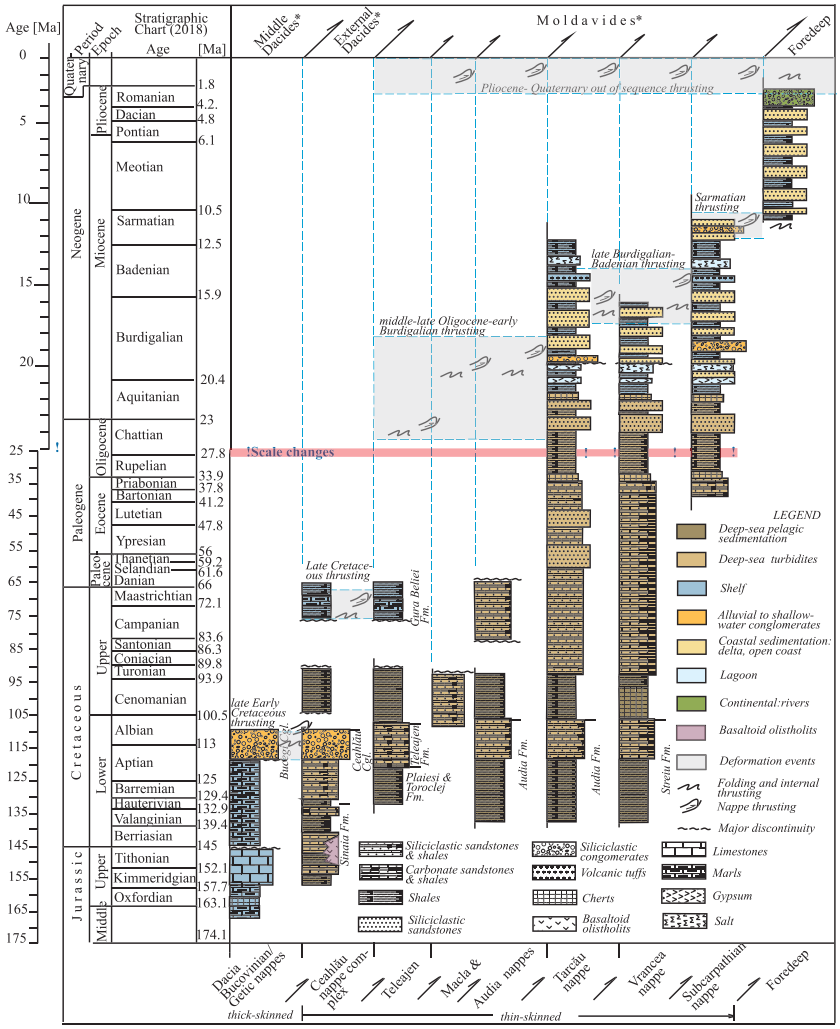

Figure 2. Simplified tectono-stratigraphic chart of the Eastern Carpathians illustrating depositional and structural relationships of the east-vergent nappes, simplified litho-stratigraphy and sedimentary environments, modified after Săndulescu et al. (1981a, 1981b); geological maps 1:50,000 and 1:200,000 published by the Geological Institute of Romania; Mațenco et al. (2007); Merten et al. (2010) and after the data presented in this study. Post-tectonic sedimentation (generally fore-arc deposition) overlying nappe contacts is not displayed.

2. Geological Setting

2.1. The Eastern Carpathians in the Regional Tectonic Framework

The Romanian segment of the Carpathians is made up by a collage of tectonic units that were gradually assembled during the closure of two main oceanic domains that are kinematically linked with the evolution of the Neotethys and Alpine Tethys (Schmid et al., 2008; Stampfli & Borel, 2002).

The Middle-Late Jurassic opening of the Ceahlău-Severin Ocean separated the Dacia tectonic mega-unit (the Bucovinian and Getic basement nappes in the studied area, or the Median Dacides of Săndulescu, 1994) to the west from the European foreland to the east (Figures 1b and 1c) (e.g., Csontos & Vörös, 2004; Săndulescu, 1988). The Early Cretaceous subduction peaked at ~110 – 100 Ma, when thrusting associated with the emplacement of these basement nappes (Iancu, Berza, Seghedi, Gheuca, & Hann, 2005a; Kräutner & Bindea, 2002) closed the Severin segment of the ocean in the Southern Carpathians and thrusted internal thrust sheets (the Baraolt and Black Flysch units) of the Ceahlău nappe system in the Eastern Carpathians (often referred to as External or Outer Dacides, Figures 1b and 1c) (Bădescu, 1997; Săndulescu, 1975; Ștefănescu, 1976). The nappe contacts of these units are often sealed by Albian shallow water to alluvial massive sandstones and conglomerates that are syn- to post-kinematic (the Ceahlău Conglomerates,

Figure 2) (Jipa & Olariu, 2018; Olariu et al., 2014; Patrulius, 1969). Given the dominant sedimentation of pelagic and deep water syn-contractional turbidites, rarely intercalated with a highly dismembered ophiolitic sequence, mostly altered basalts and dolerites observed in the Southern Carpathians, published studies generally assume that the late Middle Jurassic-Aptian sediments of the Ceahlău and Severin nappes were originally deposited in a domain characterized by oceanic crust (e.g., Bădescu, 1997; Săndulescu, 1984; Ștefănescu, 1983). Sediments deformed in all more external tectonic units of the Eastern Carpathians (the Moldavides nappes and their foredeep, Figure 2) are thought to have been deposited largely over thinned continental crust of the European passive continental margin (e.g., Roban et al., 2017; Săndulescu, 1984, and references therein). The late Early Cretaceous deformation was also associated with the eastward emplacement of a structurally higher unit that thrusted the Bucovinian and Getic basement nappe system, now found in parts of the Apuseni Mountains, in the pre-Neogene basement underlying the Transylvanian Basin and as klippen in the Eastern Carpathians. This structurally highest unit (the Transilvanides or the Eastern Vardar Ophiolites, Figures 1b and 1c) comprise ophiolitic sequences that are remnants of another ocean (the Neotethys), which was paleogeographically located west and south of the Dacia continental mega-unit (Săndulescu & Visarion, 1978, Schmid et al., 2008; see also Kounov & Schmid, 2013; Reiser et al., 2017).

Deformation peaked a second time during the latest Cretaceous (late Campanian-early Maastrichtian, ~80 – 70 Ma), when the Ceahlău nappe system was emplaced in the Eastern Carpathians over the internal part of the Moldavides. The age of this thrusting is documented by syn- to post-kinematic deposition of hemipelagic to pelagic sediments covering the nappe contacts (latest Cretaceous marine red beds of the Gura Beliei Formation, Figure 2) (Melinte-Dobrinescu & Jipa, 2007; Săndulescu, 1984). In the Southern Carpathians, coeval SE-ward directed thick-skinned thrusting of the Getic basement nappes led to the coupling with the European foreland by the incorporation of the Moesian-derived Danubian nappes in the orogenic system (Figure 1b) (e.g., Berza et al., 1983; Mațenco & Schmid, 1999; Schmid et al., 1998).

The Cretaceous stages of thrusting were followed by continued Paleogene-Neogene deformation in the Eastern and Southern Carpathians associated with up to 90° clockwise rotation of the Dacia mega-tectonic unit during its subduction of the remainder of the oceanic domain and its European passive continental margin (i.e., the Carpathians embayment) (Balla, 1986; Ustaszewski et al., 2008). The Southern Carpathians (Figure 1b) recorded a stage of Paleocene-Early Oligocene orogen-parallel extension, followed by the activation of the 100 km cumulated dextral offset along the curved Late Oligocene Cerna-Jiu and Early Miocene Timok faults systems (Figure 1b, Berza & Drăgănescu, 1988; Fügenschuh & Schmid, 2005; Kräutner & Krstić, 2002; Krézsek et al., 2013). The foredeep of the Southern Carpathians was subsequently docked by dextral transpression against the Moesian platform during Middle to Late Miocene times (the Getic Depression, Figure 1b) (Krézsek et al., 2013; Răbăgia et al., 2011). The Eastern Carpathians recorded the successive activation of the individual thin-skinned Moldavides nappes. These nappes were thrusted over various units of the Carpathians foreland and over variable distances between 140 and 180 km (Krézsek & Bally, 2006; Morley, 1996; Roure et al., 1993). Deformation peaked at times that become generally younger eastwards, from Oligocene-Early Miocene in the internal nappes, such as Teleajen (Convolute), Macla, and Audia (the Internal Moldavides of Săndulescu, 1988), earliest Miocene in the Tarcău and Vrancea (Marginal Folds) nappes, and Late Miocene in the Subcarpathian Nappe (the External Moldavides of Săndulescu, 1988), while the thin-skinned thrusting ceased at ~8 Ma (Figures 1b, 1c, and 2) (e.g., Mațenco et al., 2016; Merten et al., 2010). The contraction resumed during Pliocene-Quaternary times by thick-skinned thrusting that cross-cuts the nappe system and is restricted to the SE Carpathians area (e.g., Leever et al., 2006; Mațenco et al., 2007). This later deformation is presently active and most probably related to the evolution of high-velocity Vrancea anomaly observed beneath the SE Carpathians, interpreted to be the remnant of the Carpathians subduction slab (e.g., Ismail-Zadeh et al., 2012, and references therein). Some geophysical studies (e.g., Bokelmann & Rodler, 2014, and references therein) suggested that the seismically active Vrancea zone, associated with a positive *P* waves teleseismic mantle anomaly located beneath the southeastern Carpathians (for geometry and details, see Ismail-Zadeh et al., 2012; Martin & Wenzel, 2006), is derived from descending relict oceanic lithosphere, implying that the 140 – 180 km of Miocene shortening is related to the subduction of oceanic lithosphere. However, this suggestion is in contrast with other geophysical and geological interpretations that propose a thinned-continental origin of at least the external part of Carpathians embayment forming the European passive continental margin, (e.g., Miclăuș et al., 2009; Roban et al., 2017, and references therein).

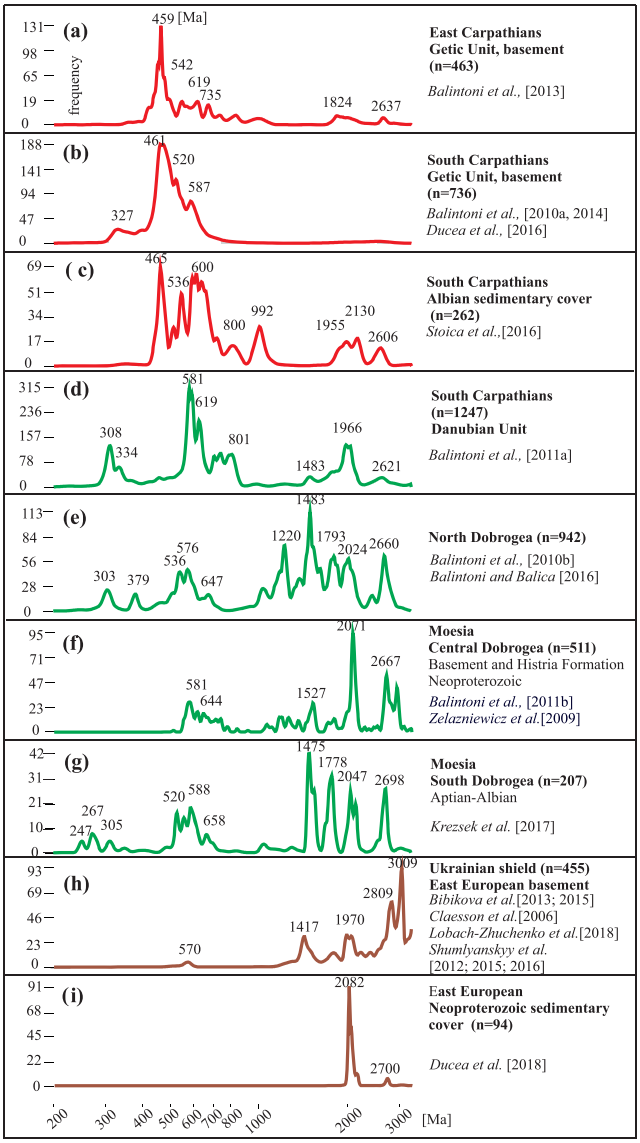

Figure 3. KDE (Kernel Density Estimate) detrital zircon age probability diagrams of Dacia tectonic mega-unit and foreland zircons compiled from various published sources. Dacia mega-unit (Getic and Bucovinic nappes) and the Albian post-tectonic cover are shown in red color (a, b, c). Danubian and foreland units are shown in green color (d, e, f, g); East European craton (h) and their sedimentary covers (i) are represented for comparison in brown.

2.2. Tectonic Evolution and Zircon Ages of Continental Units Adjacent to the Ceahlău-Severin Ocean and Its Continental Margins

Despite large gaps in quantitatively understanding the geochronology of basement rocks in the Carpathians and surrounding areas, a fairly comprehensive database of zircon provenance exists to date (see Ducea et al., 2018). This database demonstrates that the two basement units bordering both sides of the Ceahlău-Severin Ocean at the time of Early Cretaceous oceanic subduction show distinct features regarding provenance zircon radiometric ages.

The Dacia mega-unit located on the western side of the orogenic system in the current geometry (Figure 1b) consists of latest Proterozoic to Silurian island arc basement terranes metamorphosed to various degrees either immediately after their formation (Ordovician-Silurian) in the case of low grade terranes (Ducea et al., 2016) or during the Variscan orogeny in the case of higher grade rocks (Medaris et al., 2003). A Permian to Lower Cretaceous sedimentary cover overlies these units. The details regarding pre-Mesosoic island arc formation and assembly remain poorly resolved petrologically and structurally, but sufficient zircon chronology data are available (Balintoni et al., 2010b, 2014; Balintoni & Balica, 2013; Ducea et al., 2016, for a review) to fingerprint potential derivation from the Dacia mega-unit using zircon Kernel Density Estimate plots (Ducea et al., 2018) of sedimentary rocks deposited in the former Ceahlău-Severin oceanic basin. A major Ordovician peak at 458 – 472 Ma represents the culmination of a high-flux magmatic event (Stoica et al., 2016) that is distinctive for the Dacia mega-unit. Other significant zircon peaks are found at 520, 540, 580, and 600 Ma trailing toward slightly older ages (Figures 3a and 3b) but not beyond 750 Ma (Ducea et al., 2018). They may represent the ages of a nearby continental fragment or possibly the age of a thinned continental crust in which these arcs were emplaced. Older inherited zircons make up a small Grenvillian peak, and few ages older than 2.0 Ga are interpreted to have been derived from a landmass close to the island arcs. A less pronounced peak at 325 – 340 Ma indicates a Variscan event and is believed to record a period of regional metamorphism (Ducea et al., 2018). The Albian sedimentary cover of the Getic unit shows similar features (Figure 3c), having the most dominant peaks at 460 and 600 Ma, which shows a South Carpathians basement provenance (Stoica et al., 2016).

The European foreland of the eastern and southern side of the Ceahlău-Severin Ocean comprises a collage of tectonic units assembled by the end of Paleozoic times that contains a dominantly Precambrian basement overlain by a younger sedimentary cover affected by different degrees of deformation (Figures 1b and 1c). The Scythian platform, located immediately east of the Eastern Carpathians, represents the SE margin of the East European craton affected by repeated deformations during latest Proterozoic to Early Paleozoic times (Saintot et al., 2006). At farther distances to the east, from northern Crimea to north of the Caucasus, observations and detrital zircon studies demonstrate the presence of a wide Triassic volcanic arc buried below the Cenozoic sedimentary cover of the Scythian platform (Okay & Nikishin, 2015; Tikhomirov et al., 2004). The Moesian platform located south and west of the Dobrogea orogen is separated by two crustal scale faults (Figure 1b, the Intramoesian and Capidava-Ovidiu faults) into three subunits (from WSW to ENE, the Valachian, South and Central Dobrogea; Visarion et al., 1988). The Moesian platform comprises an uppermost Precambrian to lowermost Paleozoic basement exposed in Central Doborgea and contains parts of a Neoproterozoic volcanic arc, foreland basin sediments, and ophiolites (e.g., Mărunțiu et al., 1997; Oaie et al., 2005; Săndulescu, 1988; Seghedi et al., 2005). In the

Valachian part of the Moesian platform and the neighboring Balkans, older basement units are overlain by up to 4 km of Upper Cambrian-Upper Carboniferous clastic and carbonate sediments containing a Lower Paleozoic fauna that has a northern Gondwana affinity (Vaida et al., 2005). Thick Devonian turbidites and Middle-Upper Carboniferous regressive sequences are generally interpreted to be an effect of Variscan orogeny (Seghedi et al., 2005; Tari, 2005). Low amplitude deformation of the Upper Triassic-Jurassic sedimentary cover is generally interpreted to be related to a larger orogenic event associated with the closure of the Paleotethys Ocean (the Cimmerian event of Tari et al., 1997). The Central Dobrogea exposes parts of the latest Proterozoic-earliest Paleozoic Moesian basement, where low-grade greenschist facies metamorphism has affected a turbiditic to distal orogenic sedimentary sequence (Oaie et al., 2005). The North Dobrogea orogen is located between Scythia and Central Dobrogea (Moesia) and is bordered by Peceneaga-Camena and Sfântu Gheorghe faults (Figure 1b). It is exposed in North Dobrogea, continuing to the NW, beneath the Neogene cover of the Carpathians foredeep basin. This unit consists of several Cimmerian nappe structures (Săndulescu, 1984) or high-angle thrusts, which involve relics of a Variscan orogen (Seghedi, 2001; Seghedi et al., 1999, 2004) and contain metamorphic, sedimentary, and igneous rocks. The Danubian unit (included in the Marginal Dacides of Săndulescu, 1984) was part of the European margin (Moesia) and was scraped off during the Late Cretaceous deformations in response to the strong coupling between the orogen and the lower Moesian plate (Seghedi et al., 2005).

The limited data available from a few regions where this basement crops out together with subsurface data indicate that there is a common genealogy of these foreland domains that makes them at least distinctive in terms of U-Pb chronology patterns, that is, distinctive from the mobile belts found at the other end of the orogen (Dacia mega-unit). Late Variscan (250 – 310 Ma) signatures of the Danubian and the North Dobrogea units (Figures 3d and 3e) are represented by postcollisional granitoids commonly found elsewhere in the Peri Gondwanian basement of Europe (Balintoni et al., 2010a; Balintoni & Balica, 2016; Balintoni, Balica, Ducea, & Stremţan, 2011a; von Raumer et al., 2013) but not in the Dacia mega-unit, where the Variscan peak, 320 – 350 Ma, is predominantly metamorphic. The dominant age peak of the foreland units (Nord Dobrogea and Danubian) is Neoproterozoic, at 565 – 585 Ma, with progressively fewer ages toward ~800 Ma. In the Danubian tectonic unit, Neoproterozoic plutons are intruded into a metamorphosed sequence of 800 Ma old island arc rocks (Liégeois et al., 1996). Presumably, a similar scenario could be applied to less exposed units of the foreland (i.e., Moesia basement and Neoproterozoic low- to sub-greenschist facies metamorphic rocks; Figure 3f). The Aptian-Albian sedimentary cover of South Dobrogea (Figure 3g) inherits the characteristics of the basement, but also younger ages typical of post-Variscan intrusions at 245 – 255 Ma have been found in North Dobrogea (Krézsek et al., 2017). The other distinctive feature of the foreland units and North Dobrogea is the relatively abundant older ages exceeding 1 Ga (Ducea et al., 2018). The cratonic basement exposed in the Ukrainian shield is characterised by Proterozoic and Late Archean Zr ages (i.e., ~1,500, 2,000, and 2,700 Ma) (Bibikova et al., 2013, 2015; Claesson et al., 2006; Lobach-Zhuchenko et al., 2018; Shumlyanskyy et al., 2012, 2015), except some Neoproterozoic igneous intrusions (Shumlyanskyy et al., 2015) (Figure 3h). The East European Neoproterozoic sedimentary cover (Figure 3i) shows the same Archean peaks except a small Neoproterozoic one. Cambro-Silurian peaks (with a distinctive age around 465 Ma), which are common in the Getic-Bucovinian nappes, do not exist in Carpathian Foreland, Danubian, and North Dobrogea units (Ducea et al., 2018).

3. Materials and Methods

Taking into account key tectonic positions and outcrop quality, 14 localities (I to XIV) of Lower Cretaceous sediments from the thin-skinned Moldavides nappes (Figure 1b) were chosen for studies of sedimentology, anisotropy of magnetic susceptibility (AMS), petrography, and DZ U-Pb chronology (see supporting information, Figures S2, S3, and S4 and Table S1). Depositional systems were analyzed by using facies analysis principles (Miall, 2000; Walker, 1992). Source areas were analyzed at first by using paleocurrent data supplied by sedimentary structures such as flute casts (see supporting information and Table S2), corrected in stereographic projections by following the methodology of Tucker (2011). We furthermore used the anisotropy of magnetic susceptibility (AMS) at localities VIII, X, XII, XIII, and XIV (Figure 1b), where no sedimentary structures were observed. The methodology and data of this AMS analysis are presented in supporting information, Figures S5, S6, S7, and S8 and Table S3. More than 100 thin sections from Lower Cretaceous sediments and potential source areas were analyzed with a petrographic microscope Nikon

Table 1
Lithofacies Described in This Study, Occurrences, and Interpretation in Terms of Sedimentary Processes

Lithofacies	Interpretation (processes)	Localities (occurrences)													
		I	II	III	IV	V	VI	VII	VIII	IX	X	XI	XII	XIII	XIV
Shales (black)	Suspension settling (anoxic)		xxx	xxx				xxx	xxx	xxx	xxx	xxx	xxx	xxx	xx
Shales (gray)	Suspension setting (dysoxic)	x	x	x	x	x	x	x	x	x	x	x	x	x	x
Sandstones (siliciclastic, thin units)	Low-density turbidite currents	xx	x	x	xx	xx	xx	x	x	x	x	x	x	x	x
Sandstones (siliciclastic, medium and thick units)	Concentrated flow (high-density turbidite currents)	xxx			xxx	xxx	xxx				x	x	x	x	x
Sandstones (carbonate, medium and thick units)	Concentrated flow (high-density turbidite currents)													xxx	x
Gravelly sandstones (thick units)	Concentrated flow (high-density turbidite currents)	xx												x	
Breccia (thin units)	Concentrated flow (high-density turbidite currents)										x	x			
Marls and argillaceous limestones (thin units)	Suspension settling													x	xx
Siderites (lenses, nodules)	Early digenesis							x	x	x			xx	xx	x

Note. x - low frequency, xx - medium frequency, xxx - high frequency.

Eclipse 50i. Eight DZ samples (N1 to N4 and S1 to S4) were collected along two transects (see also supporrting information and Data Set S1) from the Moldavide units: a northern one in localities I, VIII, XII, and XIII and a southern one in localities V, X, XI, and XIV (Figure 1b). Along these transects, we collected one Lower Cretaceous sample from each of the Teleajen, Audia, Tarcău, and Vrancea nappes. Single zircon grains were subjected to in situ U-Pb isotopic analyses using laser ablation at the Arizona LaserChron Center, on a Nu Plasma multicollector inductively coupled plasma-mass spectrometer (LA-ICP-MS) equipped with a 193 nm Excimer laser with a beam diameter of 30 μm (Gehrels et al., 2008). We used the same workflow that is already described in Stoica et al. (2016). The extended dataset is available in the supporting information and Data Set S1. The best ages were plotted with Density Plotter (http://www.ucl.ac.uk/~ucfbpve/densityplotter/) using Kernel Density Estimate (KDE) mode and a logarithmic scale from 200 to 3,300 Ma.

4. Results and Interpretation

4.1. Lower Cretaceous Lithofacies Analysis of the Moldavides

4.1.1. Lithofacies and Sedimentary Processes

Nine types of lithofacies were separated by petrographical and sedimentological criteria as an expression of turbidity flows, suspension settling, and digenesis (Table 1).

4.1.1.1. Shales

Black shales (Figures 4a and 4b) are representative for the Hauterivian-Barremian interval in the western-most nappes of the Moldavides (localities II and III) and Valanginian-upper Albian for the eastern nappes (localities VII-XIV) (Figure 4d). These are observed as intercalations between thicker Albian sandstone levels, commonly with horizontal parallel laminations. Total Organic Carbon (TOC) ranges from 0.5% to 3% up to 8% (Balteş et al., 1984; Filipescu et al., 1966; Melinte-Dobrinescu & Roban, 2011; Roban et al., 2017; Roban & Melinte-Dobrinescu, 2012). The Hauterivian to Aptian interval is mainly composed of shales inter-bedded with thin sandstones (Figure 4b), while gray shales are associated with black shales and sandstones within the Albian (Figure 4c). These shales suggest pelagic or hemipelagic suspension settling in anoxic or dysoxic environment.

4.1.1.2. Sandstones

Thin (max. 10 cm) (Figures 4a and 4g), medium (max. 30 cm) (Figure 4d), to thick (max. 250 cm) sandstones were observed (Figure 4f). The Hauterivian-Aptian interval is dominated by lithic thin siliciclastic

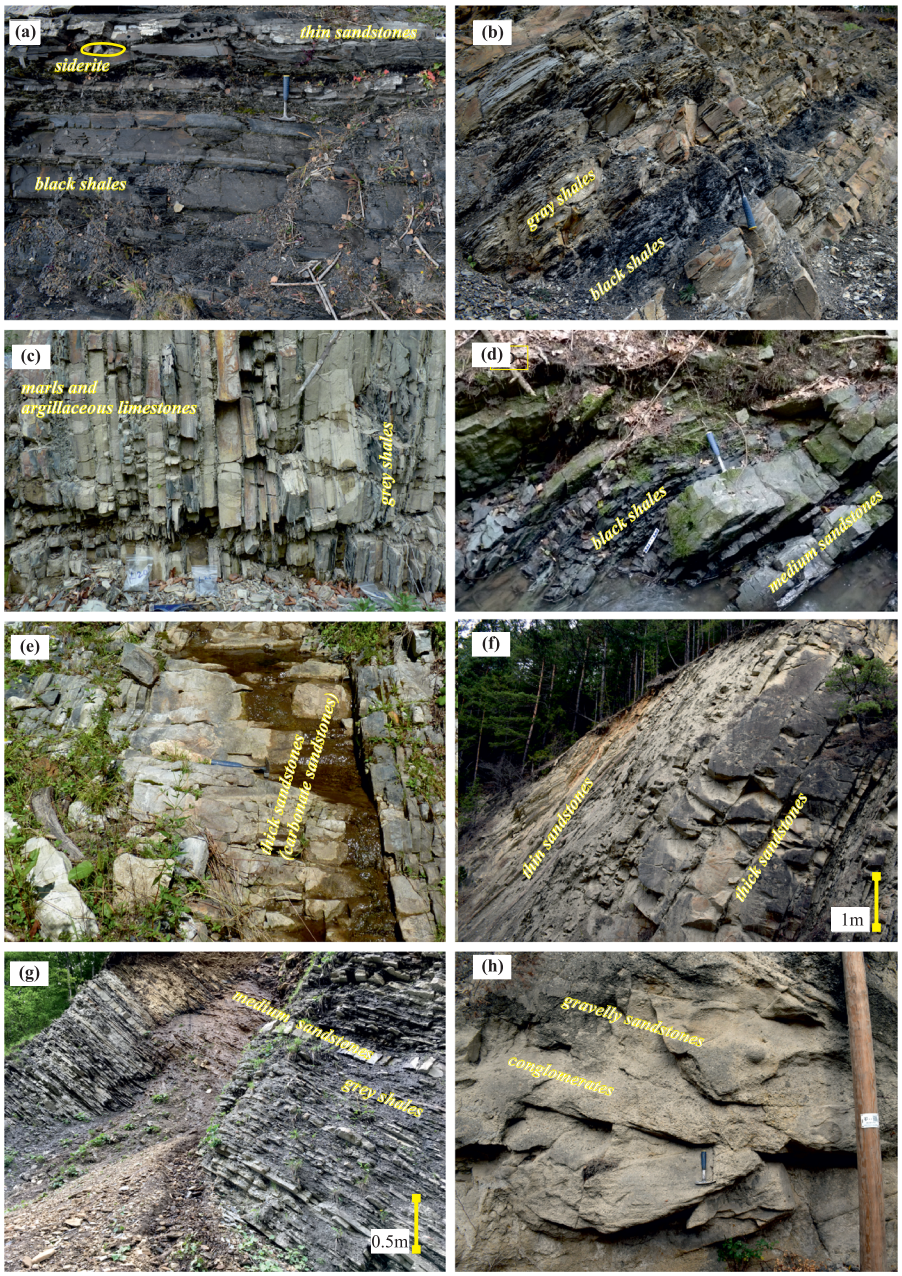

Figure 4. Lower Cretaceous lithofacies associations of the nappes of Moldavides thin-skinned thrust and fold belt. (a) Association A, basin floor sheets and lobe fringes intercalations, Audia Nappe, Barremian (location XII), black and gray shales, siderites, and thin sandstones; (b) Association A, Audia Nappe, Aptian, (location VIII), black and gray shales; (c) Association B, basin floor sheets and lobe fringes, Vrancea Nappe, Albian (location XIV), marls, argillaceous limestones, and gray shales; (d) Association D, turbidite lobes or frontal splays, Audia Nappe, Albian (location X), sandstones, black and gray shales; (e) Association E, calcareous turbidite channels and levees, Vrancea Nappe Albian, (location XIII); (f) Association F, siliciclastic turbidite channels and levees, Teleajen Nappe, Albian (location I); (g) Association F, levees, Teleajen Nappe, Albian (location VI); (h) Association G, gravely sandstone turbidite channels, Teleajen Nappe, Albian. All key locations labelled with Roman letters are marked in Figure 1.

sandstones having horizontal parallel and ripple cross laminations (I, II, and VI). These are the expression of low-density turbidite currents (sensu Lowe, 1982). The Albian quartzous sandstones and graywackes in the central studied area (localities VIII, IX, X, XI and XII) are up to 1 m thick (Figure 3d). The Albian decimeters thick carbonate sandstones (Figure 4e) from the eastern part of the Moldavides are rich in bioclasts. In the

western part, the lithic sandstones are thicker, up to 250 cm (Figure 4f). Massive and water escape structures suggest granular flows (Lowe, 1982) or hypeconcentrated density flows (sensu Mulder & Alexander, 2001). Normal grading of medium and thick sandstones suggests concentraded density flow (Mulder & Alexander, 2001) or high-density turbidite flow (Lowe, 1982).

4.1.1.3. Conglomerates

These are observed in the western part of Moldavides, that is, the Albian of the Teleajen Nappe (locality I). Grain size varies from gravel to sandy gravel or gravelly sand, where metamorphic and carbonate clasts are abundant. The thickness is up to few meters (Figure 4h). The internal unorganized structure is the result of hypeconcentrate density flows. The normal grading or large-scale cross stratification suggests high-density turbidite currents. In the eastern Moldavides, some Albian decimeter-thick conglomerate (locality XIII) bearing green clasts of schists are the result of high-density turbidite currents.

4.1.1.4. Breccias

This lithology is scarce, but rather intriguing due to its unusual composition. In the Aptian-Albian of the Audia Nappe (localities X and XI) centimeter-thick breccia levels with angular clasts are composed mainly of red granodiorites, rhyolites, basalts, and limestones. These levels are associated with black and gray shales and even with the upper part of quartzous sandstone beds. Beside chaotic structure, a crudely normal grading was observed (Figure 8e). In the eastern part of the Moldavides, the Aptian of the Vrancea Nappe (locality XIII) is characterized by few centimeter-thick levels of lens shape, rich in green metamorphic and carbonate clasts. The normal grading tendency suggests a turbulent component of flow, while the association with shales suggests a mixed hydrodynamic genesis. A close intrabasinal source area of a continental basement was interpreted to supply the observed lithic red fragments (Grigorescu & Anastasiu, 1976; Murgeanu, 1937).

4.1.1.5. Marls and Argillaceous Limestones

Centimeter-thick layers of this lithology dominate the Albian deposition in the eastern part of Moldavides (locality XIV) (Figure 4c). The $CaCO_3$ ranges from 35% to 70%. Beside carbonates, illite, chlorite, quartz, albite, and feldspars observed (Roban et al., 2017). Some levels are abundant in carbonate bioclasts. These features suggest hemipelagic and pelagic suspension settling.

4.1.1.6. Siderites

Lenses (Figure 4a) or bed shapes of decimeter-thick siderite occur in the Valanginian-Barremian interval in the eastern part of Moldavides, (localities VIII, IX, X, XII, XIII and XIV). In these rocks, the Fe_2O_3 ranges from 25 to 30%, (Grasu et al., 1988; Melinte-Dobrinescu & Roban, 2011; Roban & Melinte-Dobrinescu, 2012). The siderite is observed as cement around the siliciclastic or carbonate grains. This cementation is a secondary effect during the early diagenesis stage in a methanic nonsulphidic environment (Berner, 1981), associated to the black shale deposition.

4.1.2. Lithofacies Associations and Sedimentary Architecture

Seven types of Lower Cretaceous lithofacies associations were interpreted for a deep-sea deposition in basin plain sheets, turbiditic lobes, and channels (Table 2).

Association A dominates the Valanginian-Aptian interval in the eastern (localities VII–XII) and easternmost Moldavide nappes (localities XIII and XIV, Figure 1b). A typical section is presented in Figure 5, log A, and details are shown in Figures 4a and 4b (locality XII, Figure 1b). The section of Figure 5, log A, mainly exposes black and gray shales, thin sandstone intercalations, and siderites. The shale-sandstone ratio varies from 3:1 to 9:1. In the Aptian, the percentage of gray shales increases, while the siderite content decreases. This association is interpreted in terms of basin plain sheets with lobe fringes (sensu Mutti & Ricci-Lucchi, 1972; Walker, 1992) or frontal splays (sensu Sprague et al., 2005; Posamentier & Walker, 2006) intercalations, where the thin sandstones increase in abundance.

Association B is representative for the Albian of the Vrancea nappe in the eastern part of the Moldavides (locality XIV, Figure 1b; Figures 4c and 5, log B). It contains black shales, marls, and some argillaceous limestones with bioclasts. The centimeter-thick, sometimes decimeter-thick, sandstone intercalations are rare. The association is characteristic for basinal plain sheets with frontal splays influences (Roban et al., 2017).

Association C is also specific for the eastern part of the Moldavides such as observed in the Vrancea nappe (locality XIV, Figure 1b) and was observed within the Hauterivian-Aptian interval. This association is made by black and gray shales and thin sandstones. The percentage of thick sandstones is higher when compared with Association A. The shale/sandstone ratio varies from 1:1 to 4:1 (Figure 5, log C).

Table 2
Identified Lithofacies Associations, Their Occurrences and Architectural Interpretation

Lithofacies associations	Interpretation (architecture)	Localities (occurrences)													
		I	II	III	IV	V	VI	VII	VIII	IX	X	XI	XII	XIII	XIV
A (mainly black shales and thin sandstones)	Basin floor sheets and lobe fringes (frontal splays) of mud-rich and mixed (mud and sand) fans (mainly anoxic)		x	x				x	x	x	x	x	x	x	
B (mainly gray shales, marls and thin sandstones)	Basin floor sheets and lobe fringes (frontal splays) of mud-rich and mixed (mud and sand) fans (mainly dysoxic to oxic)														x
C (thin sandstones, black and gray shales)	Basin floor sheets and crevasse splays of mud-rich and mixed (mud and sand) fans (mainly anoxic)														x
D (thin to medium sandstones and black shales)	Lobes or frontal splays of mixed (mud and sand) fans								xx	xx	x	x	xx		
E (mainly medium to thick carbonate sandstones and gray shales)	Channels and levees of mixed (mud and sand) fans													x	
F (thin to medium sandstones and gray shales)	Channels and levees of sandy fans	x	x		x	x									
G (mainly thick gravelly sandstones)	Channels of sandy fans	x					x								

Note. x - low frequency, xx - medium frequency, xxx - high frequency.

The presence of small channels and slumps suggests lower slope to basin floor environments, levee, and crevasse splay architectures.

Association D is typical for the Albian of the Audia and Tarcău Nappes (localities VIII, IX, X, XI, and XII; Figure 1b). It consists of decimeter- to occasionally meter-thick sandstones with black and gray shales interlayered with thin sandstones. The sandstones are massive or normal graded (Figure 5, log D), while the centimeter- to decimeter-thick ones show cross-laminations. This association is typical for the architecture of turbiditic lobes or frontal splays of basin floor channels (sensu Posamentier & Walker, 2006).

Association E (Figures 4e and 5, log E) was observed within Albian deposits in the northern part of the Vrancea nappe (locality XIII, Figure 1b). At the base of the decimeter-thick massive or normal graded carbonate sandstones or carbonate sandstone, rare conglomerates are present. The intercalations occurring between massive sandstones are composed of thin sandstones but also black and gray shales. These deposits of high-density turbiditic currents indicate the transition from slope to basin floor channels and levee.

Association F is typical for the Albian sediments of the innermost (western) nappe of the Moldavides, that is, the Teleajen unit (localities I, II, IV, V, and VI; Figure 1b). In this association, fining-upwards sequences of decimeter- up to meter-thick massive or normal graded sandstones and conglomerates at the base occur, capped by cross-laminated and convolute centimeter-thick sandstones, alternating with black and gray shales (Figures 4f, 4g, and 5, log F). These sequences are typical for slope channel fill and levee architectures.

Association G has a restricted areal occurrence (locality I, Figure 1b), in the northern part of the Teleajen nappe (Figures 4h and 5, log G), having 60–70 m stratigraphic thickness in deposits of upper Aptian-upper Albian age. It contains clast to matrix-supported conglomerates to coarse sandstones, mainly situated in metric organized units with normal grading and cross stratifications. These characteristics suggest a submarine channel fill.

The overall correlations between the composite sections across each tectonic nappe interpretations are presented in Figure 6. This correlation shows a significantly larger thickness of the Aptian-Albian deposits in the westernmost Moldavides unit, that is, in the Teleajen Nappe.

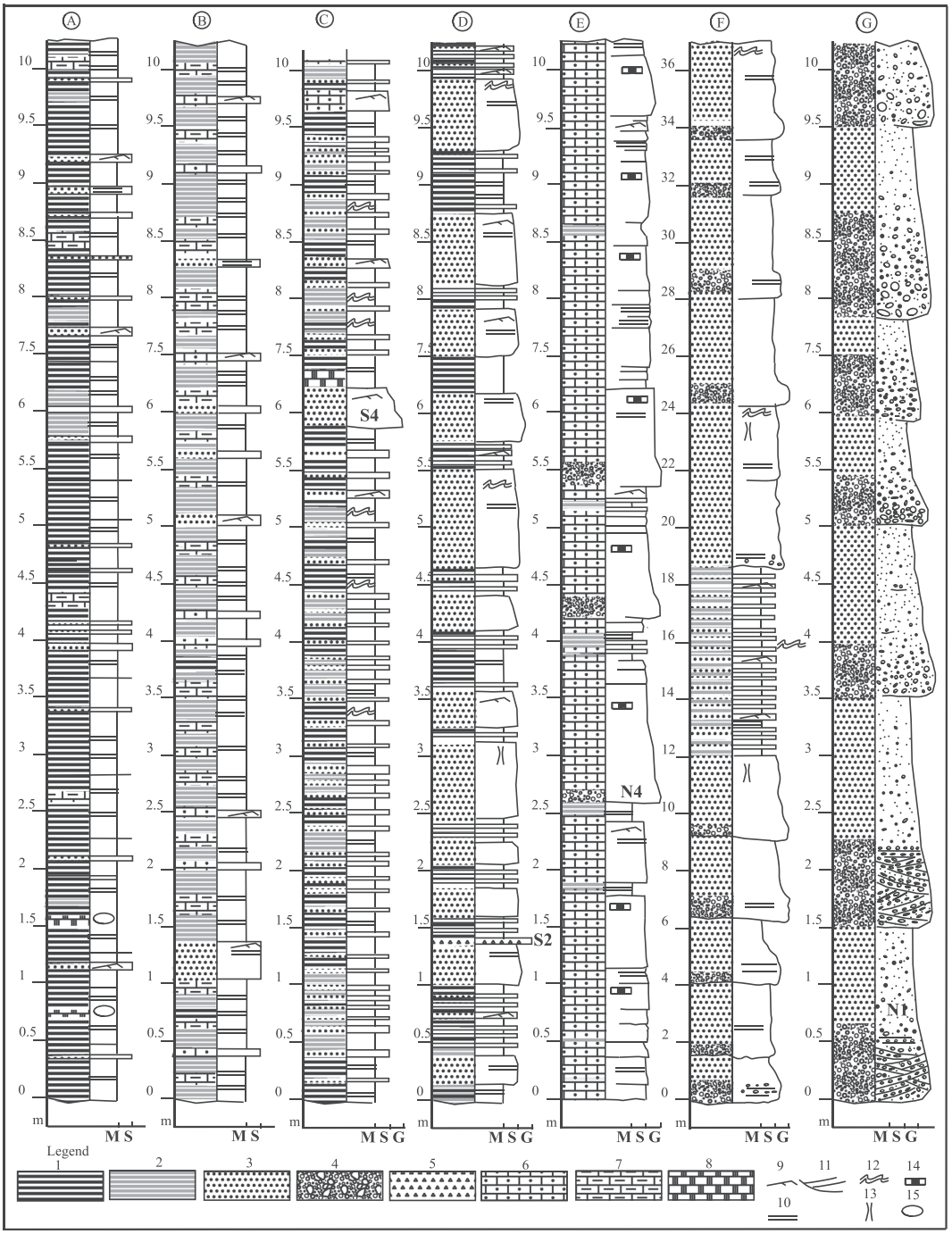

Figure 5. Sedimentary logs of encountered lithofacies associations. (A) basin floor sheets and lobe fringes or frontal splays, Vrancea Nappe, Valanginian-Aptian (location XII); (B) carbonate rich basin floor sheets and lobe fringes, Vrancea Nappe, Albian (location XIII); (C) Basin floor sheets and crevasse splays, Vrancea Nappe, Hauterivian-Aptian, Vrancea Nappe (location XIII); (D) siliciclastic turbidite lobes or frontal splays, Audia Nappe, Albian (location X); (E) carbonate rich turbidite channels and lobes, Vrancea Nappe, Albian (location XIII); (F) Siliciclastic turbidite channels and levees, Teleajen Nappe, Albian (location VII); (G) turbidite siliciclastic channels, Teleajen Nappe, Albian (location I). M - mud; S - sand; G - gravel. Legend: 1 - black shales; 2 - gray shales; 3 - sandstones; 4 - conglomerates; 5 - breccia; 6 - carbonate sandstones; 7 - marls; 8 - siderites; 9 - ripple laminations; 10 - horizontal parallel laminations; 11 - large scale cross stratifications; 12 - deformational convolute laminations; 13 - water escape structures, 14 - diagenetic silicifications; 15 - diagenetic nodules. All key locations labelled with Roman letters are marked in Figure 1. S4, S2, N4, and N1 indicate the position of the DZ samples.

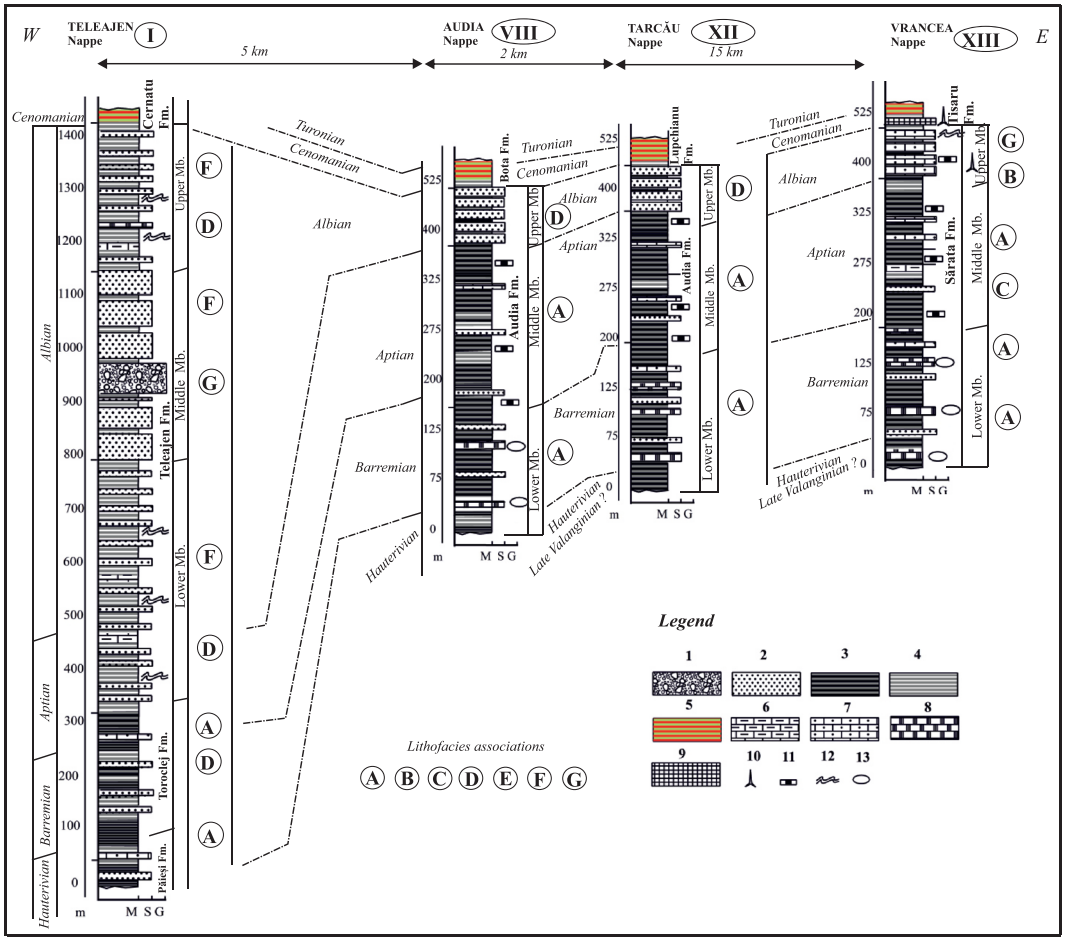

Figure 6. Composite sedimentary lithological logs for the nappes of the Moldavides representing lithofacies associations (capital letters) explained in Figure 4, for the Valanginian-Turonian interval. Legend: 1 - conglomerates; 2 - sandstones; 3 - black shales; 4 - gray shales; 5 - red and green shales; 6 - marls; 7 - carbonate sandstone; 8 - siderites; 9 - cherts, radiolarites; 10 - sponge spicules; 11 - diagenetic silicification; 12 - deformational convolute laminations; 13 - diagenetic nodules (siderites). All key locations labelled with Roman letters are marked in Figure 1.

4.2. Paleocurrent Data and Petrography

4.2.1. Paleocurrent Analysis

4.2.1.1. Teleajen Nappe (Westernmost Moldavides)

As shown in Figure 7, the Hauterivian-Aptian sedimentary structures (mostly flute casts) from lobe fringe associations (locality III) indicate transport directions towards ESE (average azimuth 100°). At locality II, the Aptian flute casts indicate transport directions towards ESE (average azimuth 110°). The Albian channel fills deposits from locality I indicate transport directions towards NE (average azimuth 45°), while the levees show mainly NNW directions (azimuth 350°). The Albian flute casts from channels from locality IV indicate transport directions towards ESE currents (azimuth 110°), while the levees are directed to ENE (azimuth 75° – 80°).

4.2.1.2. Audia and Tarcău Nappes (Central Part of the Moldavides)

The Hauterivian-Aptian flute casts and ripples cross-laminations indicate transport directions towards south in locality VII (azimuth 170° – 190°, Figure 7), while in locality XII the AMS data indicate SW directions (azimuth 220°, supporting information, Figure S5). In the northern part (locality VII), the directions of the Albian flute casts in the turbiditic lobe associations indicate transport directions towards S and SSW (azimuths 182° and 192°). The AMS data from locality VIII indicate WNW direction (azimuth 280°; see also supporting information, Figure S6). In the southern sector of the Eastern Carpathian (locality X, supporting

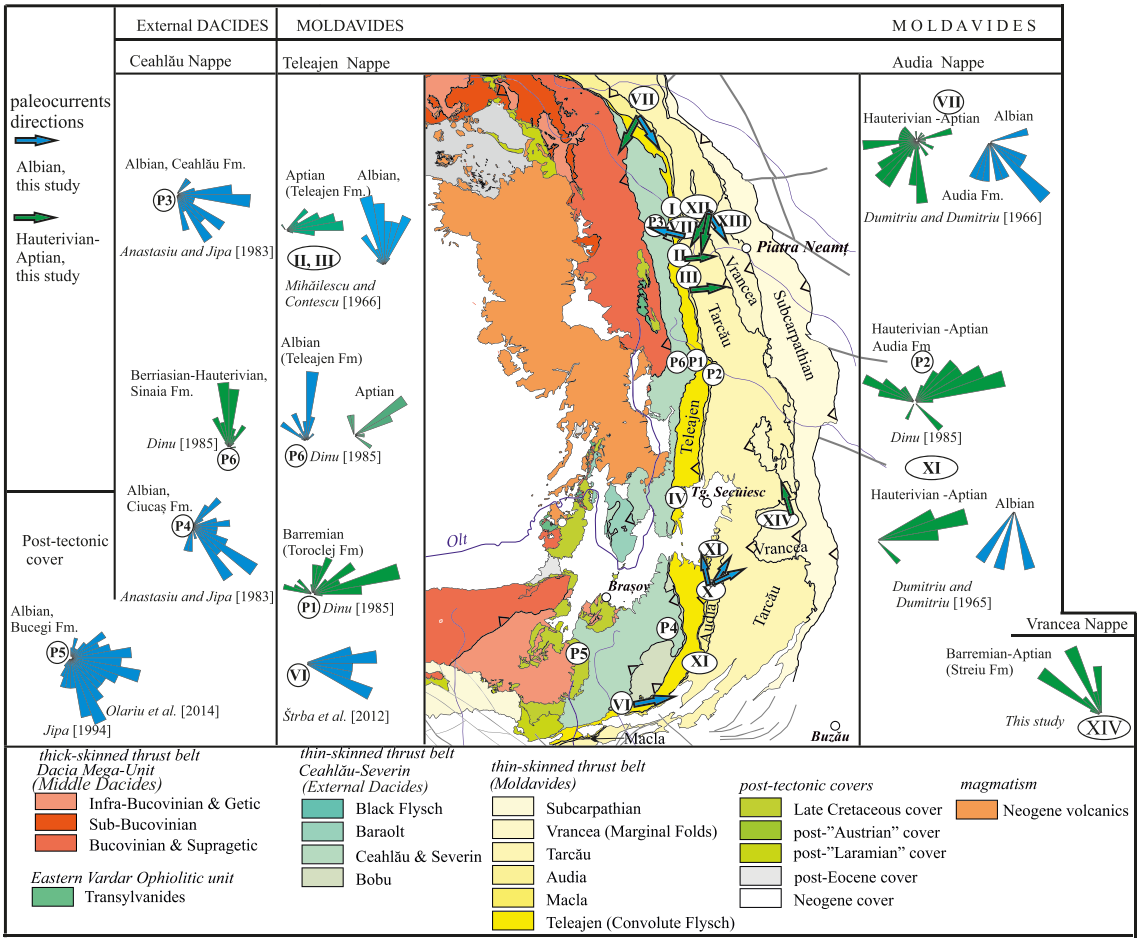

Figure 7. Map showing paleocurrents directions within the thin-skinned thrust belt of the Eastern Carpathians (Moldavides nappes) and a compilation of literature data (rose diagrams displayed to the left and the right of the map). The arrows in the map denote data derived from sedimentary structures and the anisotropy of magnetic susceptibility (AMS) measured during this study. I - Teleajen Nappe, Albian; II - Teleajen Nappe, Aptian; III - Teleajen Nappe, Barremian; IV - Teleajen Nappe, Aptian-Albian; VII - Audia Nappe, Hauterivian-Albian; VIII - Audia Nappe, Hauterivian-Albian; IX - Audia Nappe, Hauterivian, Abian; X - Audia Nappe, Albian; XII - Tarcău Nappe, Albian; XIV - Vrancea Nappe, Berriasian-Albian. The localities for the histograms based on the data procured from the Moldavides are as follows: P1 - Teleajen Nappe, Hauterivan-Albian; P2 - Audia Nappe, Hauterivian-Aptian; and those from the External Dacides are: P3 - Ceahlău Conglomerates, Ceahlău Nappe, Albian; P4 - Ciucaș Conglomerates, Ceahlău Nappe, Albian; P5 - Bucegi Conglomerates, Albian; P6 - Ceahlău Nappe, Berriasian. All key locations labelled with Roman letters are marked in Figure 1 and some of the histogms showing literature data refer to the areas around these key locations.

information, Figure S8), the Albian sedimentary structures indicate a higher dispersion pattern, the transport directions being mainly oriented towards NE and NW (azimuth 50°, 75°, and 340°).

4.2.1.3. Vrancea Nappe (Eastern Moldavides)

We have measured sedimentary structures in one location in this eastern part of the Moldavides (locality XIV, Figure 7), where the Barremian-Aptian lobe fringes associations indicate transport directions towards N and NW (azimuth 280° to 350°, Figure 7; see also supporting information, Figure S7). These data are also confirmed by AMS measurements (azimuth 352°-2°). Neither measurable sedimentary structures nor conclusive AMS data were observed or measured in Albian sediments.

4.2.2. Petrography and Detrital Zircon (DZ) U-Pb Chronology

Aptian-Albian sandstones were analysed for determining whether they were sourced from the Dacia mega-units or the European foreland, as well as to shed light upon their supposed intrabasinal source.

4.2.2.1. Teleajen Nappe (Westernmost Moldavides)

Sample N1 was collected from a turbiditic channel fill complex in Albian sediments (locality I, Figure 1b) of the northern part of the Teleajen Nappe (Figures 4h and 5, log G). Petrographically, it is a matrix-supported conglomerate made up of round to subround granules and pebbles, up to 2 cm in size. Lithic clasts comprise

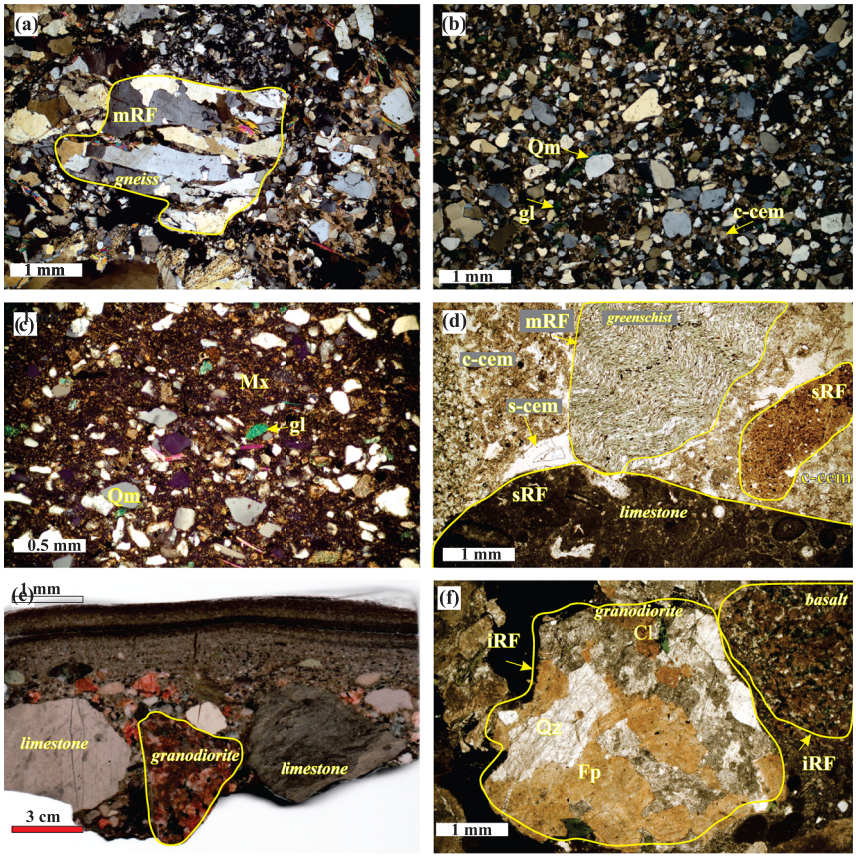

Figure 8. Petrotypes of samples used for U-Pb DZ analysis. (a) Sample N1 (location I), Albian conglomerate, Teleajen Nappe; (b) Sample N2 (locationVIII), Audia Nappe, Albian quartzous sandstone, carbonate cement and phyllosilicate matrix; (c) Sample N3 (location XII), Tarcău Nappe, Albian quartzous/lithic graywacke bearing glauconite, phyllosilicate matrix with recrystallized silica. (d) Sample N4 (location XIII), Albian carbonate sandstone bearing greenschist clasts; (e) Hand specimen S3 (location XI), breccia level with red granodiorite, Audia Nappe, Albian/Aptian. Alongside red clasts, limestones, marls and weathered basalts appear; (h) Close-up of a red clast, granodiorite with altered plagioclase feldspars stained with iron oxide (Sample S2). On the right, a highly weathered basalt fragment with chloritized glass. mRF = metamorphic rock fragment; sRF = sedimentary rock fragment; iRF = igneous rock fragment; Qm = monocristaline quartz, Fp = plagioclase feldspars; Mx = matrix, gl = glauconite; s-cem = siliceous cement; c-cem = carbonate cement. All key locations labelled with Roman letters are marked in Figure 1.

K-feldspar gneisses, schists, and rarely sedimentary carbonate rock fragments (Figure 8a). The grains are monocrystalline and polycrystalline quartz, muscovite, biotite, chloritized biotite, and heavy minerals such as garnets and zircons. The 99 separated zircon grains have a distinctive peak at 457 Ma and other two at 532 and 614 Ma, with an insignificant number of grains older than 1 Ga. The age distribution probability density curve has two small peaks at 308 and 340 Ma (Figure 9a).

Sample S1 was collected from Albian sediments of the southern part of the Teleajen Nappe (locality V, Figure 1b), which comprises metric sandy turbiditic channels. The sample is made up by fine to medium subrounded lithic sandstones, containing monocrystalline quartz, micas, and subordinate feldspars. Lithic fragments are sparse and of metamorphic origin. The sample contains both carbonate and phyllosilicate cement, as well as a clay-based matrix. Out of the 97 zircons, the age distribution is very similar to that of sample N1 described above. The most prominent peak in sample S1 is at 462 Ma, then gradually decreases in frequency, with other peaks at 599 and 789 Ma (Figure 9b).

4.2.2.2. Audia and Tarcău Nappes (Central Part of the Moldavides)

S*ample N2* was taken from the northern Audia Nappe and is a quartzous sandstone with a turbiditic lobe architecture (locality VIII, Figure 1b). It is a massive, fine- to medium-grained arenite with poor parallel lamination observed in its upper parts. Subordinate minerals are mica and peloid glauconite (Figure 8b). DZ analyses on 103 zircons yield an age range from 234 to 2,600 Ma. The maximum peak is at 326 Ma,

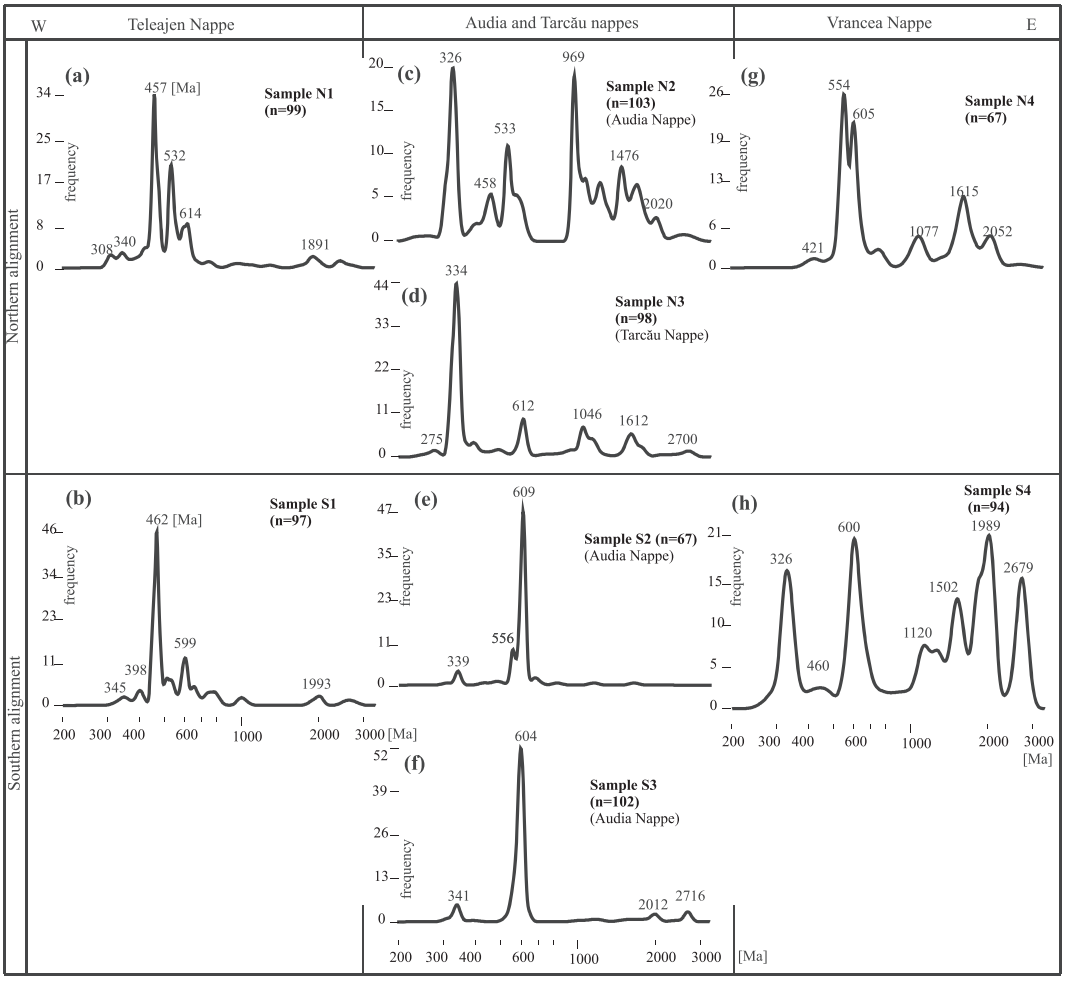

Figure 9. Kernel Density Estimate (KDE) of U-Pb age distribution of detrital zircons (DZ) from the thin-skinned Moldavides thrust belt of the Eastern Carpathians. (a) Sample N1, Teleajen Nappe, Albian conglomerate (location I); (b) Sample S1, Teleajen Nappe, Albian sandstone location (V); (c) Sample N2, Audia Nappe, Albian sandstone (location VIII); (d) Sample N3, Tarcău Nappe, Albian graywacke (location XII); (e) Sample S2, Audia Nappe, Aptian-Albian, breccia level with red clasts, (location X); (f) Sample S3, Audia Nappe, breccia level with red clasts (location XI); (g) Vrancea Nappe, Sample N4, Aptian-Albian, carbonate sandstone bearing gravely greenschist clasts (XIII); (h) Sample S4, Vrancea Nappe, Aptian-Albian sandstone (location XIV). All key locations labelled with Roman letters are marked in Figure 1.

while others are clustered at 402, 458, and 533 Ma. Less prominent peaks are found at 969, 1,219, 1,476, 1,714, and 2,020 Ma (Figure 9c).

Sample N3 is an Albian turbidite lobe from the northern region of the Tarcău Nappe (locality XII, Figure 1b). It is compositionally similar to sample N2, with a siliceous and phyllosilicate matrix containing calcite granular aggregates (Figure 8c). Glauconite makes up as much as 7%. DZ spectrum consisting of 98 zircon grains is dominated by a 334 Ma peak. Secondary peaks are found at 612, 1,046, and 1,612 Ma (Figure 9d).

Samples S2 and S3 are from the southern region of the Audia Nappe. Aptian-Albian breccia levels with red clasts were found at two locations, approximately 100 km apart, S2 in locality X, and S3 in locality XI (Figure 1b). The facies association is that of turbidite lobes. The sample was taken from a massive to normal grading polymict breccia with plutonic, metamorphic, volcanic, and sedimentary rock fragments (Figure 8e). The matrix is made up of phyllosilicates, but there is a significant amount of calcite cement. An abundance of celadonite cement was observed, formed from volcanic clast weathering. Plutonic lithic fragments are composed of granodiorites with weathered iron oxide stained plagioclase (Figure 9f). There are frequent intergrowths between quartz and K feldspar. Volcanic clasts consist of basalts partly

chloritized and weathered feldspar. Gneissic clasts often show chloritized biotite. Samples contain also fragments of Jurassic limestone with Calpionellids and marl fragments. Both samples showed almost identical DZ age patterns, with a maximum peak at 604 and 609 Ma and a subordinate peak at ~340 Ma (Figures 9e and 9f).

4.2.2.3. Vrancea Nappe (Eastern Moldavides)

Sample N4 was collected from the northern region of the Vrancea Nappe from the Albian channel-levees associaltion. The sample is a normal graded clast-supported conglomerate containing predominantly clasts of greenschists (Figures 5, log E, and 8d) and metagraywacke or metasiltstone fragments, both with secondary chlorite. Some fragments appear deformed, while others do not show any deformation. There are also micrite limestone fragments as well as carbonate bioclasts. Typical occurrences are sponge spicules and silicification. The cement consists of carbonate with abundant pyrite. The 67 analyzed zircons have peaks at 554 and 605 Ma. Secondary peaks are visible at 1,079, 1,615, and 2,052 Ma (Figure 9g).

Sample S4 was collected from an Aptian sandstone located in the southern part of the Vrancea Nappe (Figures 1b and 5, log C). It is a laminated sandstone containing phyllosilicate minerals, single grain quartz, and abundant lithic fragments of low-grade metamorphic. Micrite limestone, carbonate fossils, silt sedimentary rocks, and graywackes fragments are also found. Glauconite is common, and the cement is carbonatic. Siderite forms some crystals clusters. The DZ age range is broad, with peaks at 600 and 326 Ma. Other significant are peaks at 1,120, 1,502, 1,989, and 2,679 Ma (Figure 9h).

Most zircons from all the samples have U/Th < 5 and are thus of igneous origin (Hoskin & Schaltegger, 2003). However, there are some DZ peaks in both the Carboniferous (320 – 340 Ma) and Ordovician (450 – 470 Ma) populations (Figures 10a, 10b, 10c, 10d, and 10h) that are of metamorphic origin. These findings are in agreement with existing data, which demonstrate both Ordovician and Carboniferous metamorphism in the Dacia mega-unit (Ducea et al., 2016; Medaris et al., 2003).

5. Discussion

The combined sedimentological and detrital zircon analyses demonstrate that the studied Lower Cretaceous sediments presently exposed in the Moldavides thin-skinned belt of the Eastern Carpathians have been sourced from both the Dacia mega-unit basement and from the European foreland. Given the 140 – 160 km minimum original width of the Moldavides basin (Figure 11) prior to the Miocene shortening (Krézsek & Bally, 2006; Morley, 1996; Roure et al., 1993), it is likely that the Early Cretaceous sedimentation took place in a narrow basin, where paleobathymetries were in the 600 – 2,500 m range (Melinte-Dobrinescu et al., 2015). This previous inference is in agreement with recent regional quantitative Mediterranean reconstructions that account for the kinematics of nappe emplacement in the Carpathians (Figures 12a and 12c) (van Hinsbergen et al., 2020). These reconstructions assume the existence of a wide passive continental margin during the Early Cretaceous, which was connected with the European foreland units and was subducted (Figures 11a and 11b) or accreted to the Dacia tectonic upper plate during the subsequent Late Cretaceous-Miocene tectonic events (e.g., Mațenco, 2017; Mațenco et al., 2010; Săndulescu, 1988).

5.1. Audia-Vrancea Deep-Sea Depositional System Supplied by the European Foreland

The European passive continental margin accommodated low energy, mostly pelagic sedimentation during the Valanginian-Aptian, in a domiprovidednantly anoxic environment, particularly well observed in the external (eastern) Audia, Tarcău, and Vrancea nappes. Basin floor sheets with thin lobe fringes intercalations of muddy-rich submarine fans (Association A) (Figure 11a), with a high dispersion pattern of paleocurrents (Figures 12a and 12b) are typical in the distal part of the basin relative to the European foreland source areas. Crevasse splays of basin floor channels are also common in the more proximal eastern and southern sectors (Association C).

Turbidite lithofacies of sandy-mud fans were more abundant in the Albian (Figures 11b, 11c, and 12d). In addition to basin floor associations (Associations A and B), typical carbonate sandstones dominating channels and levee associations (Association E) are common in the proximal eastern area of the Moldavides basin and are most likely supplied by a mixed carbonate-siliciclastic source. In the more distal sectors, siliciclastic lobes or frontal splays of sandy mud fans (Association D) might be connected to the siliciclastic delta systems of the European foreland, possibly during sea-level low stands.

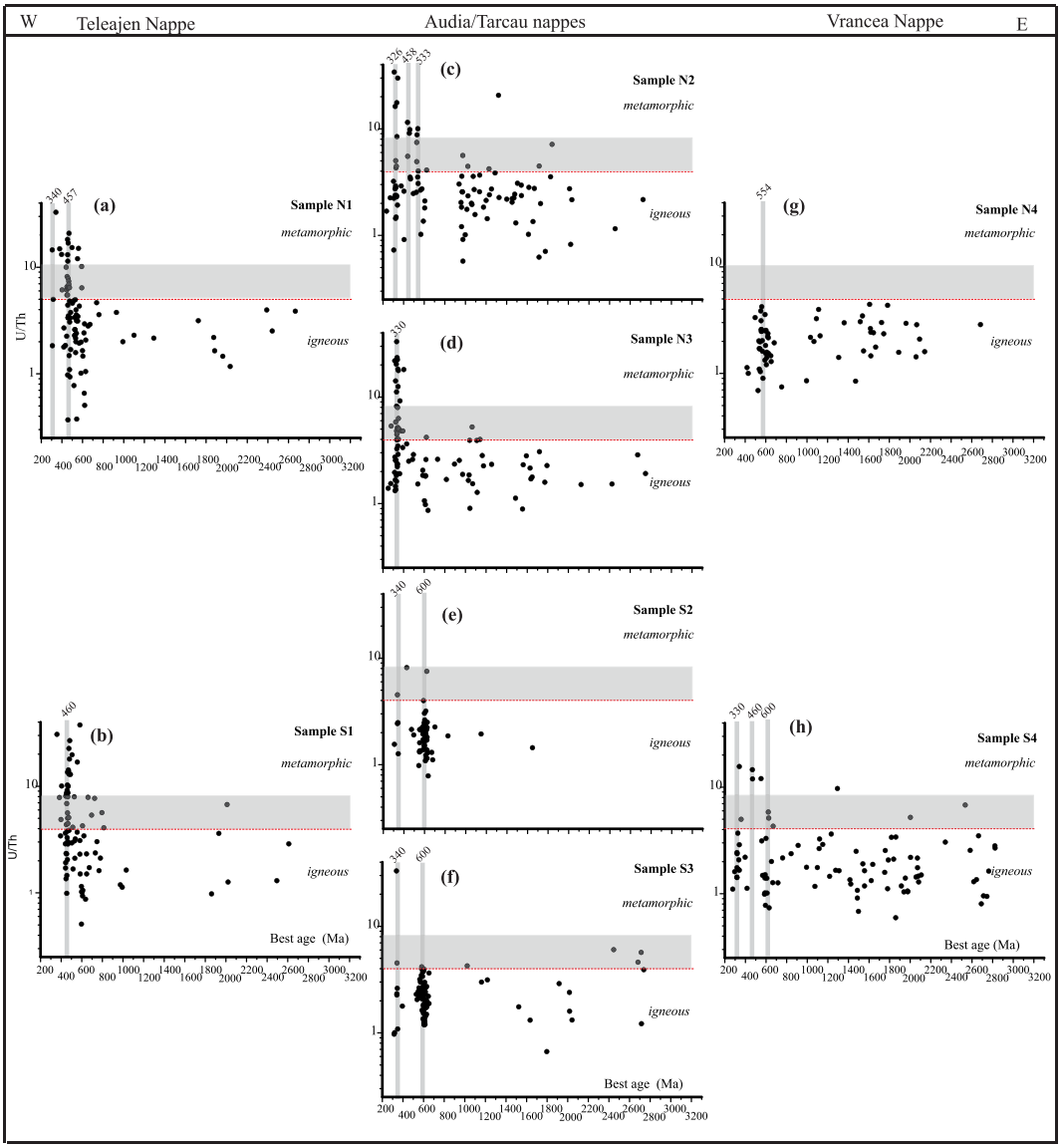

Figure 10. U/Th ratios of the samples used for DZ. U/Th < 5 are of igneous origin. (a) Sample N1, Teleajen Nappe, Albian conglomerate (location I); (b) Sample S1, Teleajen Nappe, Albian sandstone (location V); (c) Sample N2, Audia Np., Albian sandstone, (VIII); (d) Sample N3, Tarcău Nappe, Albian graywacke, (location XII); (e) Sample S2, Audia Nappe, Aptian-Albian, breccia level with red clasts, (location X); (f) Sample S3, Audia Nappe, breccia level with red clasts, (location XI); (g) Vrancea Nappe, Sample N4, Aptian-Albian, carbonate sandstone bearing gravely greenschist clasts (location XIII); (h) Sample S4, Vrancea Nappe, Aptian-Albian sandstone (location XIV). All key locations labelled with Roman letters are marked in Figure 1.

Beyond the evidence provided by paleocurrent directions (Figures 7, 12a, 12c), eastern European foreland sources are also evident from petrographic composition and DZ ages of analyzed samples. The abundance of the Albian sandstones bearing greenschist clasts of low metamorphic grade and sedimentary carbonate fragments in the external Vrancea Nappe (Figure 8d) suggests an European foreland provenance (Anastasiu, 1984). The main DZ peaks of the analyzed samples from Audia, Tarcău, and Vrancea nappes are at 320–340 Ma and 570–610 Ma, but also Precambrian ages between 1 and 2 Ga are relatively common. The 570–610 Ma peak is best exemplified by the exposures of the Danubian basement in the South Carpathians (Figure 3d) (Balintoni, Balica, Ducea, & Stremţan, 2011a) and North Dobrogea (Figure 3e) (Balintoni & Balica, 2016). The correlation is valid because, paleogeographically, the Danubian unit was part of Moesia before the late Early Cretaceous (e.g., Seghedi et al., 2005, and references therein) and, therefore, belongs to the European foreland. Furthermore, many other areas of the European foreland contain the same age cluster: Neoproterozoic deposits of Histria Formation in the Central Dobrogea that consist of

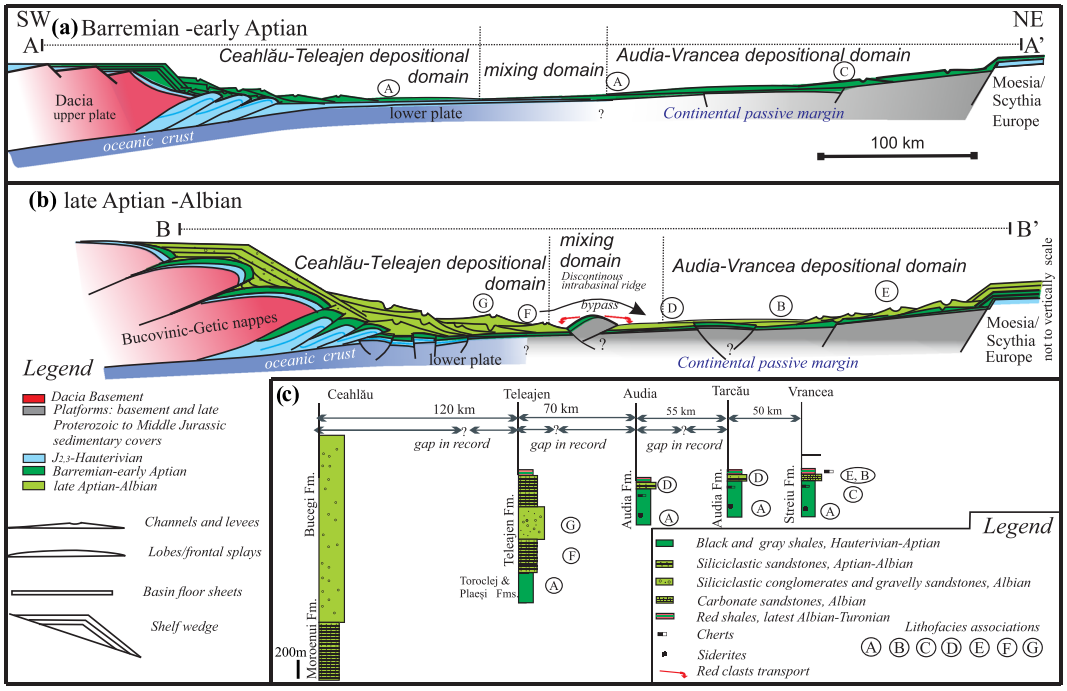

Figure 11. Cross-section sketch reconstructions of the Ceahlău-Severin Ocean and its continental passive margin showing depositional systems during Barremian-Aptian and Albian. (a) Reconstruction of the depositional systems for the Barremian-Aptian interval. The western area depicts Barremian to early Aptian sandy turbiditic systems having the Dacia mega-unit as their source area, overliying the deposits of the acretionary wedge formed by the sediments of the Ceahlău-Severin Ocean (Middle Jurassic to Hauterivian). The eastern area shows muddy turbiditic systems, levees, crevasse splay and distal turbidite lobes sourced from the European foreland; (b) Reconstruction for late Aptian-Albian time when the Dacia mega-unit further overthursts the deposits of the Ceahlău-Severin Ocean creating a major subsidence that leads to the formation of sandy and gravelly depositional systems (Bucegi, Ciucaş conglomerates and Teleajen Formation). The eastern part depicts sandy-mud rich fans with channels and levees and distal turbidite lobes that have a European source. See Figures 12a and 12c for the location of sections A–A′ and B–B′; (c) lithological logs of Lower Cretaceous deposits from the Moldavides (Vrancea, Tarcău, Audia, and Teleajen nappes) correlated with the Lower Cretaceous of the Middle and External Dacides. The distance between the logs are calibrated by balanced cross-section reconstructions in the Eastern Carpathians (Krézsek & Bally, 2006; Roure et al., 1993).

low-grade metamorphic schists (Figure 3f) (Balintoni et al., 2011b; Oaie et al., 2005; Zelazniewicz et al., 2009) and the Albian sedimentary cover from South Dobrogea, which is also part of the Moesian platform (Figure 3g) (Krézsek et al., 2017, and references therein).

Proterozoic and late Archean peaks (i.e., ~1,500, 2,000, and 2,700 Ma) found in the eastern Moldavides nappes are characteristic for the foreland units of the Carpathian orogen: the East European platform basement (Figure 3h), the East European Neoproterozoic sedimentary cover (Figure 3i), the Moesian platform (Figure 3f), and North Dobrogea (Figure 3e). The igneous and metamorphic Carboniferous peaks of 320 – 340 Ma (Figures 10a, 10b, 10c, 10d, 10e, and 10h) are rare among the studied basement of the Carpathians and foreland units of Romania (Ducea et al., 2018) but are characteristic for some other areas of the mobile Paleozoic Europe, such as the igneous rocks from the Bohemian Massif (Jastrzębski et al., 2018), among several others. This interval, broadly referred to as Variscan, is when major Barrovian collisional metamorphim took place in the Dacia mega-unit and contains only limited, low temperature leucogranitic magmatism (Balintoni et al., 2014). Potential sources for this magmatic peak are either yet to be resolved plutons in the basement (poorly covered by geochronologic studies) or a higher basement thrust sheet (potentially now eroded) in the Dacia mega-unit. Notably, these 320 – 340 Ma ages are also found in the Jurassic sandstones of the Moesian platform (*G. Tari* personal communication to M. Ducea), suggesting thus a foreland origin of this Variscan magmatic event.

An intrabasinal “Cuman” ridge or uplifted areas situated between Teleajen and Audia depositional sectors (Figures 11b and 12d) have long been interpreted to provide local sources along the European passive continental margin (Grigorescu & Anastasiu, 1976; Murgeanu, 1937), in order to explain the provenance of exotic red granodiorite clasts dominating the thin breccia levels of the Aptian-Albian deposits from the Audia

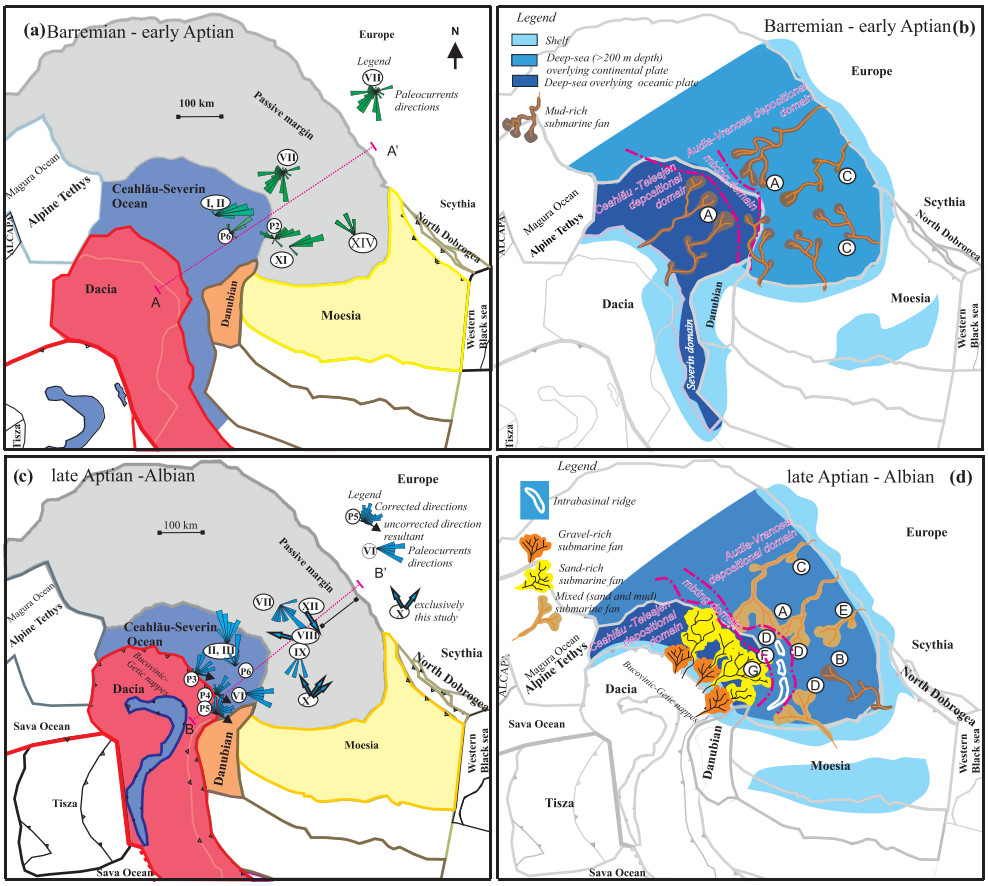

Figure 12. Sedimentary system reconstruction for the Barremian-Albian in the Romanian Carpathians area. The tectonic reconstruction of continental units, oceans, and passive margins is re-drawn from van Hinsbergen et al. (2020). (a) Ceahlău-Severin Ocean, European passive continental margin and surrounding units: Dacia mega-unit and European foreland. Paleocurrents directions during the Barremian-early Aptian time; (b) Paleogeographical reconstruction and location of the Barremian-lower Aptian muddy-rich fans; (c) The paleocurrent directions during late Aptian-Albian; (d) Gravel and sand-rich fans supplied by the Dacia mega-unit and the sand-muddy rich fans sourced from the European foreland. The paleocurrent directions for the Bucegi (P5), Ciucaş (P4), and Ceahlău (P3) conglomerates were corrected considering the post Albian clock-wise rotation of the Dacia block (~90°). The traces of sections A–A′ and B–B′ refer to the profiles in Figure 11. The key locations labelled with Roman letters are marked in Figures 1 and 7. A, B, C, and so forth refer to the litofacies associations shown in Figure 5. The paleogeographical reconstruction of the surrounding area is after Świdrowska et al. (2008) - East European and Scythian platforms and Costea et al. (1978) - Moesian platform.

Nappe of the Moldavides (localities X and XI) (Figures 8e and 8f). The S2-S3 samples from these breccia levels have a DZ age distribution with a ~600 Ma peak, which is most likely associated to the foreland units rather than the Dacia basement nappes (Figures 9e and 9f). The same samples also contain a 340 Ma peak. This compositional mixing between granodiorite-rich breccias with angular basalt fragments, weathered trachytes of unknown origin, or age and Upper Jurassic-Lower Cretaceous limestones infers reworking of Mesozoic sediments and a direct provenance from the Moesian basement. The postulated ridge was either a rift horst (possibly inverted) or was generated by flexural bulging of the lower plate in response to Cretaceous thrusting events. The same red granodiorite fragments were found locally in the southern area of Teleajen Nappe, supporting the location of a ridge in the area between Audia and Teleajen units. The interpretation of such intrabasinal sources is not unique in the Carpathians. Many continental fragments or ridges have been interpreted in the Western Carpathains (e.g., Czorsztyn and Silesian) with a relatively similar structure (Golonka et al., 2006; Oszczypko, 2006; Plašienka, 2018). The Silesian Ridge was active starting with the Upper Cretaceous and contains gneissic fragments with a peak DZ age of 530–570 Ma and Albian sandstones with a peak DZ age of 600 – 630 Ma, as well as distinctive older peaks from 1,250 to 2,740 Ma (Budzyń et al., 2011; Michalík et al., 2006), not found in the internal Carpathian units such as the Dacia Block. These data suggest an European origin of both Silesian and Cuman ridges. However, this intrabasinal ridge interpretation is still speculative simply

because it cannot completely exclude far transported high-density turbidites deposited from an external European foreland source or from temporary storage areas situated in a more distal position relative to this foreland, similar with what is observed in other turbidite systems (e.g., Postma et al., 2014; Strachan et al., 2013).

5.2. Ceahlău-Teleajen Deep-Sea Depositional Systems Supplied by Dacia Mega-Unit

The low energy pelagic sedimentation and muddy turbidite systems found along the European passive continental margin were laterally replaced in the western part of the basin, located close to the subduction zone beneath the Dacia continental unit (i.e., the Ceahlău-Teleajen depositional domain in Figures 12b and 12d), by high energy channels and levees (Associations F and G) of the sandy systems, deposited during late Aptian-Albian times, as observed in the Teleajen nappe (Figures 11b, 11c, and 12d). Our data demonstrate that source areas of these Teleajen nappe deposits were exclusively those of the basement of the Dacia continental mega-unit, which is in concordance with previously published paleocurrent data (Figures 7 and 12c) (Anastasiu & Jipa, 1983; Dinu, 1985; Mihăilescu & Contescu, 1966; Štrba, 2012). The DZ of the two Albian samples (Figures 9a and 9b) from the Teleajen Nappe are dominated by igneous and metamorphic Ordovician peaks (460 Ma), characteristic for the basement of the Getic nappes of the Dacia continental mega-unit (Ducea et al., 2018) (Figures 3a and 3b). These source areas were likely reactivated by the closure of the Severin ocean segment in the South Carpathians (Figures 11b, 11c, and 12d) and the Cretaceous thrusting of the Dacia thick-skinned napes over the inner part of the Ceahlău nappe sediments in the case of the Eastern Carpathians (Iancu, Berza, Seghedi, Gheuca, & Hann, 2005a; Kräutner & Bindea, 2002; Săndulescu, 1994). This thrusting has exhumed the basement of the Dacia unit and the internal-most part of the Ceahlău accretionary wedge (e.g., Merten et al., 2010; Sanders et al., 1999), while more external parts of this wedge were overlaid by the thick sequences of gravel-rich submarine fans (Figures 11b, 11c, and 12d) of Bucegi (locality P5), Ciucaș (locality 4), and Ceahlău (locality P3) conglomerates (Figure 12c) (Olariu et al., 2014). The restoration of previously published paleocurrent directions (Figure 7) (Anastasiu & Jipa, 1983; Dinu, 1985; Jipa, 1994; Jipa & Olariu, 2018; Olariu et al., 2014) by the post-Cretaceous 90° clockwise rotations of the Dacia mega-unit (Figure 12c) demonstrates that the gravel-rich submarine fans were laterally connected with the more distal high-density sandy turbidite systems observed in the Teleajen Nappe (see also Figures 11b, 11c, and 12d). It is likely that the overall contractional event created both flexural loading and subsidence in the lower plate combined with uplift and high rates of erosion in the thrusting front of the Dacia nappes. We were not able to identify an intrabasinal source area located west of the Teleajen depositional domain for the high-density turbiditic fan system, such as a flexural bulge of the lower European plate, created by the late Early Cretaceous thrusting, as previously proposed (e.g., Bădescu, 2005; Săndulescu, 1984). The dominant U-Pb ages for the Dacia sourced Teleajen nappe sediments suggests that the Albian conglomeratic system overlying the internal part of the accretionary wedge was rather directly connected with the turbiditic system of the Teleajen nappe in the original depositional domain (Figures 11b and 12d).

5.3. Mixing of Sources

The distribution of paleocurrents during the Hauterivian-Barremian interval in the internal Teleajen Nappe (Figures 1 and 7, locality P1) and during the Valanginian-Aptian time in the more external Audia and Tarcău nappes (Figures 1 and 7, localities VIII and P2) show opposite transport directions, both to the E and W. Since these directions were measured in the basin floor sheet and turbidite frontal splay or lobe fringe association, the high grade of dispersion is understandable (Figure 12b). Alternatively, the opposite directions could suggest different source areas and turbidite systems mixing the sediments in the middle part of the basin (Figure 12b).

During the Albian, the internal Teleajen Nappe of the Moldavides shows that paleocurrents from channels and levee associations had N and NW orientations (Figures 7 and 12c, localities I, II, P6), while in the external Audia and Tarcău nappes, the frontal splay associations indicate southward directions in the northern sector (Figures 7 and 12c, localities VII, XII, IX) and northward directions in the southern one (Figures 7 and 12c, locality X). These data suggest the convergence and alignment of currents in the median sector of the basin parallel to the strike of the Albian thrust belt in the west. In the deposits sourced from the European foreland, two samples (N2 and S4) show among typical European ages (330 Ma, 600 Ma, and >1 Ga) a small peak in the distribution of DZ ages at 460 Ma (Figures 9c and 9h). This observation

suggests the mixing of sediments with a different provenance, since the 460 Ma DZ age is typical of the Dacia mega-unit. Furthermore, Albian carbonate sandstones form Vrancea Nappe contain graywacke fragments (Figure 7d), typical for the Albian of Tarcău and Audia nappes (Figure 8c). However, sandstones and graywackes of Audia and Tarcău nappes contain greenschists and sedimentary carbonate fragments abundant in the more eastern Vrancea Nappe. One other possible cause of sediment mixing in the center of the basin is reworking by bottom marine currents of sediments derived from the distal turbidite facies. Therefore, we conclude that a certain degree of sediment mixing derived from both the Upper Dacia tectonic mega-unit and the lower European continental plate is observed and suggests a narrow width of the sedimentary basin.

6. Conclusions

The formation and evolution of the Eastern Carpathians thin-skinned thrust and fold belt in Central Europe has hidden, by subduction and subsequent collision, most direct evidences of the geometry of the former Ceahlău-Severin oceanic lithosphere and its attached European passive continental margin. Based on new sedimentologic, paleomagnetic, petrographic, and detrital zircon U-Pb data for Lower Cretaceous sediments cropping out in the Moldavides part of this thin-skinned belt, correlated with quantitative reconstructions of the surrounding continental units, we show that these deposits were supplied from both, the inner Dacia continental mega-unit, in an upper plate position and, from the external European foreland, located east and south of the basin. These sediments were part of a deep-sea depositional systems that overlied both the domains of oceanic lithosphere and the passive continental margin.

Although we cannot precisely quantify the extent, composition, and geometry of these domains, it is rather clear that the European foreland sourced the external Moldavides nappes (i.e., the Audia, Tarcău, and Vrancea nappes) during Valanginian-Aptian times with sediments deposited over its passive continental margin (the Audia-Vrancea depositional domain in Figures 12b and 12d). This sedimentation was low-energy, mainly pelagic settling, associated with low-density turbidite currents, while basin energy increased during the Albian, in response to the onset of Carpathians thrusting at the front of the Dacia continental mega-unit. The sourcing is demonstrated by paleocurrent directions and detrital zircon ages with peaks at 550–620 Ma and over 1 Ga, which is characteristic for the European foreland. Breccia bearing red granodiorite fragments having detrital zircon peaks at 600 Ma and 330 Ma could also be sourced by intrabasinal ridges of European origin or could have been transported at farther distances by high-density transport via intermediate storage areas.

In contrast, our study demonstrates for the first time that Lower Cretaceous sediments of the westernmost nappe attributed to the Moldavides system (i.e., Teleajen) were deposited in the immediate vicinity and to the opposite side of the basin sourced by the Dacia continental basement. These sediments must have been part of the same accretionary sedimentological system together with the more internal Ceahlău nappes. In order to differentiate this innermost part of the Modavides from the External Dacides, which refers strictly to Ceahlău-Severin nappe system, we defined a Ceahlău-Teleajen depositional domain (Figures 12b and 12d). The late Early Cretaceous thrusting changed the depositional style of sediments observed in the Teleajen Nappe to progressively higher energy sandy turbidite systems supplied by the Dacia continental basement, as indicated by paleocurrents and typical 460 Ma detrital zircon age clusters observed in Albian lithic sandstones. The relatively narrow nature of the oceanic basin during Early Cretaceous time has facilitated an occasional mixing of sources in the sediments deposited on the basin floor, as indicated by high paleocurrents dispersion and Ordovician detrital zircon ages of 460 Ma typical for the Dacia mega-unit observed in sandstones of more external Moldavides nappes.

It is important to differentiate the depositional domain of sediments from the emplacement of nappes in which these sediments are incorporated later during the evolution of thin-skinned thrust and fold belts. Despite the fact that sediments observed in the Ceahlău and Teleajen nappes were part of the same depositional system during Early Cretaceous times, Cretaceous thrusting affected only the Ceahlău nappes. Thrusting continued by foreland migration until the Oligocene-early Miocene, when the Teleajen nappe was ultimately emplaced. The latter times are also when thrusting emplaced sediments deposited in the domain of the distal European passive continental margins (Audia and Macla nappes). Deformation continued by foreland migration during the middle and late Miocene thrusting in more proximal regions of the European passive continental margins emplacing the remainder of the Moldavides nappes

(Tarcău, Vrancea, and Subcarpathian). Our findings are in agreement with the previous interpretations of a 200 – 250 km wide European passive continental margin during Early Cretaceous times that must have been subducted or accreted at high depths beneath the orogen during the subsequent Cretaceous-Miocene shortening events. This interpretation is in direct contrast with an oceanic lithosphere nature of the subducted slab beneath the southeastern Carpathians. An explanation is beyond the scope of our study, but it may be related to the exact nature of the ocean and its passive margin, such as the presence of previously not described hyper-extended continental lithosphere, or to mechanisms of subduction that still need to be investigated.

These findings demonstrate that the combination between sedimentological and provenance techniques has the ability to provide critical constraints in thin-skinned thrust and fold belts for understanding the depositional systems of subducted oceanic domains and their attached continental margins thrusted by collisional processes in areas where quantitative reconstructions of adjacent continental units are available.

Acknowledgments

This work was supported by the Project PN-II-RU-TE-2014-4-2064, No. 193/2015, and PN-III-P4-ID-PCCF-2016-0014 of the Romanian Executive Agency for Higher Education, Research, Development and Innovation, UEFISCDI. We acknowledge the support from the U.S. National Science Foundation grant EAR 1725002. We also acknowledge the financial support of the Project No. 8 PFE/FLUVIMAR, Research of Excellence in Rivers-Deltas-Seas systems of the Romanian Ministry of Research and Innovation. The Editor, Associate Editor, and reviewers provided useful guidance and suggestions to clarify concepts and problem statemens. Stefan Schmid is in particular acknowledged for the detailed revision that has significantly improved the quality of the original manuscript. The data in this paper are available in the manuscript itself or in the supplementary files: https://osf.io/qe3kb/ or DOI 10.17605/OSF.IO/QE3KB.

References

Anastasiu, N. (1984). What are the "Green clasts" of the Carpathian flysch? A petrographic reconsideration. *Revue Roumaine de Géologie Géophysique et Géographie, Academia Română*, *28*, 51–60.

Anastasiu, N., & Jipa, D. (1983). *Sedimentary textures and structures (in Romanian)* (p. 275). Bucharest, Romania: Editura tehnică.

Bădescu, D. (1997). Tectono-thermal regimes and lithosphere behaviour in the External Dacides in the Upper Triassic and Jurassic Tethyan opening (Romanian Carpathians). *Tectonophysics*, *282*, 167–188. https://doi.org/10.1016/s0040-1951(97)00218-7

Bădescu, D. (2005). *Tectono-stratigraphic evolution of the Eastern Carpathians during the Mesozoic and Cenozoic (in Romanian)* (p. 308). Bucharest, Romania: Editura Economică.

Balázs, A., Burov, E., Matenco, L., Vogt, K., Francois, T., & Cloetingh, S. (2017). Symmetry during the syn- and post-rift evolution of extensional back-arc basins: The role of inherited orogenic structures. *Earth and Planetary Science Letters*, *462*, 86–98. https://doi.org/10.1016/j.epsl.2017.01.015

Balintoni, I., & Balica, C. (2013). Carpathian peri-Gondwanan terranes in the East Carpathians (Romania): A testimony of an Ordovician North-African orogeny. *Gondwana Research*, *23*, 1053–1070. https://doi.org/10.1016/j.gr.2012.07.013

Balintoni, I., & Balica, C. (2016). Peri-Amazonian provenance of the Euxinic Craton components in Dobrogea and of the North Dobrogean Orogen components (Romania): A detrital zircon study. *Precambrian Research*, *278*, 34–51. https://doi.org/10.1016/j.precamres.2016.03.008

Balintoni, I., Balica, C., Ducea, M., & Stremţan, C. (2011a). Peri-Amazonian, Avalonian-type and Ganderian-type terranes in the South Carpathians, Romania: The Danubian domain basement. *Gondwana Research*, *19*, 945–957. https://doi.org/10.1016/j.gr.2010.10.002

Balintoni, I., Balica, C., Ducea, M. N., & Hann, H. P. (2014). Peri-Gondwanan terranes in the Romanian Carpathians: A review of their spatial distribution, origin, provenance and evolution. *Geoscience Frontiers*, *5*, 395–411. https://doi.org/10.1016/j.gsf.2013.09.002

Balintoni, I., Balica, C., Ducea, M. N., Hann, H. P., & Sabliovschi, V. (2010a). The anatomy of a Gondwanan terrane: The Neoproterozoic-Ordovician basement of the pre-Alpine Sebeş-Lotru composite terrane (South Carpathians, Romania). *Gondwana Research*, *17*(2–3), 561–572. https://doi.org/10.1016/j.gr.2009.08.003

Balintoni, I., Balica, C., Seghedi, A., & Ducea, M. (2011b). Peri-Amazonian provenance of the Central Dobrogea terrane (Romania) attested by U/Pb detrital zircon age patterns. *Geologica Carpathica*, *62*(4), 299–307. https://doi.org/10.2478/v10096-011-0023-x

Balintoni, I., Balica, C., Seghedi, A., & Ducea, M. N. (2010b). Avalonian and Cadomian terranes in North Dobrogea, Romania. *Precambrian Research*, *182*, 217–229. https://doi.org/10.1016/j.precamres.2010.08.010

Balla, Z. (1986). Paleotectonic reconstruction of the central Alpine–Mediterranean belt for the Neogene. *Tectonophysics*, *127*, 213–243. https://doi.org/10.1016/0040-1951(86)90062-4

Balteş, N., Antonescu, E., Grigorescu, D., Alexandrescu, G., & Micu, M. (1984). The Black Shale Formation of the East Carpathians, lithostratigraphy and oil potential. *Anuarul Institutului de Geologie şi Geofizică*, *59*, 79–88.

Berner, R. A. (1981). A new geochemical classification of sedimentary environments. *Journal of Sedimentary Petrology*, *51*, 359–365. https://doi.org/10.1306/212F7C7F-2B24-11D7-8648000102C1865D

Berza, T., & Drăgănescu, A. (1988). The Cerna-Jiu fault system (South Carpathians, Romania), a major Tertiary transcurrent lineament. *Dări de Seamă ale Institutului de Geologie şi Geofizică*, *72-73*(5), 43–57.

Berza, T., Kräutner, H., & Dimitrescu, R. (1983). Nappe structure in the Danubian window of the Central South Carpathians. *Anuarul Institutului de Geologie şi Geofizică*, *LX*, 31–39.

Bibikova, E. V., Claesson, S., Fedotova, A. A., Stepanyuk, L. M., Shumlyansky, L. V., Kirnozova, T. I., et al. (2013). Isotope-geochronological (U-Th-Pb, Lu-Hf) study of the zircons from the Archean magmatic and metasedimentary rocks of the Podolia domain, Ukrainian shield. *Geochemistry International*, *51*(2), 87–108. https://doi.org/10.1134/S0016702913020031

Bibikova, E. V., Fedotova, A. A., Claesson, S., & Stepanyuk, L. M. (2015). Early crust of the Podolia domain of the Ukrainian shield: Isotopic age of terrigenous zircons from quartzites of the Bug Group. *Stratigraphy and Geological Correlation*, *23*(6), 555–567. http://doi.org/10.1134/S0869593815060027

Bokelmann, G., & Rodler, F.-A. (2014). Nature of the Vrancea seismic zone (Eastern Carpathians)—New constraints from dispersion of first-arriving P-waves. *Earth and Planetary Science Letters*, *390*, 59–68. https://doi.org/10.1016/j.epsl.2013.12.034

Budzyń, B., Dunkley, D. J., Kusiak, M. A., Poprawa, P., Malata, T., Skiba, M., & Paszkowski, M. (2011). SHRIMP U-Pb zircon chronology of the Polish Western Outer Carpathians source areas. *Annales. Societatis Geologorum Poloniae*, *81*, 161–171.

Bush, M. A., Horton, B. K., Murphy, M. A., & Stockli, D. F. (2016). Detrital record of initial basement exhumation along the Laramide deformation front, southern Rocky Mountains. *Tectonics*, *35*, 2117–2130. https://doi.org/10.1002/2016TC004194

Claesson, S., Bibikova, E., Bogdanova, S., & Skobelev, V. (2006). Archaean terranes, Palaeoproterozoic reworking and accretion in the Ukrainian Shield, East European Craton. In D. Gee, & R. A. Stephenson (Eds.), *European Lithosphere Dynamics* (pp. 645–654). London: Geological Society London Memoirs.

Contescu, L. R. (1974). Geologic history and paleogeopraphy of Eastern Carpatians: Example of Alpine geosynclinal evolution. *American Association of Petroleum Geologists Bulletin*, *58*, 2436–2475. https://doi.org/10.1306/83d91bcd-16c7-11d7-8645000102c1865d

Costea, I., Comșa, D., & Vinogradov, C. (1978). Microfaciesurile cretacicului inferior din Platforma Moesică. *Studii și Cercetări Geologice, Geofizice, Geografice, Geologie*, *23*(2), 299–311.
Csontos, L., & Vörös, A. (2004). Mesozoic plate tectonic reconstruction of the Carpathian region. *Paleogeography Paleoclimatology and Paleoecology*, *210*, 1–56. https://doi.org/10.1016/j.palaeo.2004.02.033
DeCelles, P. G., Ducea, M. N., Kapp, P., & Zandt, G. (2009). Cyclicity in Cordilleran orogenic systems. *Nature Geoscience*, *2*, 251–257. https://doi.org/10.1038/ngeo469
Dinu, C. (1985). Geologic study of the Cretaceous flysch deposits in the upper course of the Trotuș Valley (East Carpathians). *Anuarul Institutului de Geologie și Geofizică*, *65*, 5–142.
Ducea, M., Giosan, L., Carter, A., Stoica, A. M., Roban, R. D., Balica, C., et al. (2018). U-Pb detrital zircon geochronology of the lower Danube and its tributaries; implications for the geology of the Carpathians. *Geochemistry, Geophysics, Geosystems*, *19*, 3208–3223. https://doi.org/10.1029/2018GC007659
Ducea, M. N., Negulescu, E., Profeta, L., Săbău, G., Jianu, D., Petrescu, L., & Hoffman, D. (2016). Evolution of the Sibișel Shear Zone (South Carpathians): A study of its type locality near Rășinari (Romania) and tectonic implications. *Tectonics*, *35*, 2131–2157. https://doi.org/10.1002/2016TC004193
Favre, P., & Stampfli, G. M. (1992). From rifting to passive margin: The example of the Red Sea Central Atlantic and Alpine Tethys. *Tectonophysics*, *215*, 69–97. https://doi.org/10.1016/0040-1951(92)90075-H
Filipescu, M. G., & Alexandrescu, G. (1962). *Distribution of coarse-grained sandstones and arkoses with red feldspars in the Cretaceous of the Eastern Carpathians, Studii și Certetări de Geologie* (Vol. VII, pp. 241–248). Bucharest, Romania: Editura Academiei RPR.
Filipescu, M. G., Botez, C., Olaru, D., Donos, M., & Donos, I. (1966). Chimismul șisturilor negre de pe Valea Covasna. *Analele Științifice ale Universității Al I. Cuza Iași*, *6*(2), 34–44.
Fügenschuh, B., & Schmid, S. M. (2005). Age and significance of core complex formation in a much curved orogen: Evidence from fission track studies in the South Carpathians (Romania). *Tectonophysics*, *404*, 33–53. https://doi.org/10.1016/j.tecto.2005.03.019
Gaina, C., Torsvik, T. H., van Hinsbergen, D. J. J., Medvedev, S., Werner, S. C., & Labails, C. (2013). The African Plate: A history of oceanic crust accretion and subduction since the Jurassic. *Tectonophysics*, *604*, 4–25. https://doi.org/10.1016/j.tecto.2013.05.037
Gehrels, G. E., Valencia, V. A., & Ruiz, J. (2008). Enhanced precision, accuracy, efficiency, and spatial resolution of U-Pb ages by laser ablation–multicollector–inductively coupled plasma–mass spectrometry. *Geochemistry, Geophysics, Geosystems*, *9*, Q03017. https://doi.org/10.1029/2007GC001805
Golonka, J., Gahagan, L., Krobicki, M., Marko, F., Oszczypko, N., & Ślączka, A. (2006). Plate-tectonic evolution and Paleogeography of the Circum-Carpathian Region. In J. Golonka, & F. J. Picha (Eds.), *The Carpathians and their foreland: Geology and hydrocarbon resources* (Vol. 84, pp. 11–46). AAPG Memoir. http://doi.org/10.1306/985606M843066
Grasu, C., Catană, C., & Grinea, D. (1988). *Carpathian flysch. Petrography and economic considerations* (p. 208). Bucharest, Romania: Editura Tehnică.
Grigorescu, D., & Anastasiu, N. (1976). Coarse-grained clastic constituents of Cretaceous deposits from the black shales unit: Sedimentological significance. *Studii și Cercetări Geologice, Geofizice și Geografice, Seria Geologie*, *21*, 95–102.
Handy, M. R., Schmid, S. M., Bousquet, R., Kissling, E., & Bernoulli, D. (2010). Reconciling plate-tectonic reconstructions of Alpine Tethys with the geological-geophysical record of spreading and subduction in the Alps. *Earth-Science Reviews*, *102*(3-4), 121–158. https://doi.org/10.1016/j.earscirev.2010.06.002
Hoskin, P. W. O., & Schaltegger, U. (2003). The composition of zircon and igneous and metamorphic petrogenesis. *Reviews in Mineralogy and Geochemistry*, *53*(1), 27–62. https://doi.org/10.2113/0530027
Iancu, V., Berza, T., Seghedi, A., Gheuca, I., & Hann, H.-P. (2005a). Alpine polyphase tectono-metamorphic evolution of the South Carpathians: A new overview. *Tectonophysics*, *410*(1–4), 337–365. https://doi.org/10.1016/j.tecto.2004.12.038
Iancu, V., Berza, T., Seghedi, A., & Maruntiu, M. (2005b). Palaeozoic rock assemblages incorporated in the South Carpathian Alpine thrust belt (Romania and Serbia): A review. *Geologica Belgica*, *8*(4), 48–68. https://popups.uliege.be/1374-8505/index.php?id=772
Ismail-Zadeh, A., Mațenco, L., Radulian, M., Cloetingh, S., & Panza, G. (2012). Geodynamics and intermediate-depth seismicity in Vrancea (the south-eastern Carpathians): Current state-of-the art. *Tectonophysics*, *530–531*, 50–79. https://doi.org/10.1016/j.tecto.2012.01.016
Jastrzębski, M., Machowiak, K., Krzemińska, E., Farmer, G. L., Larionov, A. N., Murtezi, M., et al. (2018). Geochronology, petrogenesis and geodynamic significance of the Visean igneous rocks in the Central Sudetes, northeastern Bohemian Massif. *Lithos*, *316–317*, 385–405. https://doi.org/10.1016/j.lithos.2018.07.034
Jipa, D. (1994). *The study of lateral sedimentation, PhD Thesis* (p. 230). University of Bucharest.
Jipa, D. C., & Olariu, C. (2018). Significance of the Bucegi Conglomerate olistoliths in the Albian source-to-sink system from the Carpathian Bend basin in Romania. *Interpretation*, *6*(1), 29–37. https://doi.org/10.1190/int-2017-0030.1
Kounov, A., & Schmid, S. (2013). Fission-track constraints on the thermal and tectonic evolution of the Apuseni Mountains (Romania). *International Journal of Earth Sciences*, *102*, 207–233. https://doi.org/10.1007/s00531-012-0800-5
Kräutner, H. G., & Bindea, G. (2002). Structural units in the pre-Alpine basement of the Eastern Carpathians. *Geologica Carpathica*, *53*, 143–146.
Kräutner, H. G., & Krstić, B. (2002). Alpine and Pre-Alpine structural units within the Southern Carpathians and the Eastern Balkanides. *Geologica Carpathica*, *53*, 1–7.
Krézsek, C., & Bally, A. W. (2006). The Transylvanian Basin (Romania) and its relation to the Carpathian fold and thrust belt: Insights in gravitational salt tectonics. *Marine and Petroleum Geology*, *23*, 405–442. https://doi.org/10.1016/j.marpetgeo.2006.03.003
Krézsek, C., Bercea, R. I., Tari, G., & Ionescu, G. (2017). Cretaceous sedimentation along the Romanian margin of the Black Sea: Inferences from onshore to offshore correlations. In M. D. Simmons, G. C. Tari, & A. I. Okay (Eds.), *Petroleum geology of the Black Sea* (Vol. 464, pp. 211–245). London: Geological Society of London, Special Publication. https://doi.org/10.1144/SP464.10
Krézsek, C., Lăpădat, A., Mațenco, L., Arnberger, K., Barbu, V., & Olaru-Florea, R. (2013). Strain partitioning at orogenic contacts during rotation, strike–slip and oblique convergence: Paleogene–Early Miocene evolution of the contact between the South Carpathians and Moesia. *Global and Planetary Change*, *103*(1), 63–81. https://doi.org/10.1016/j.gloplacha.2012.11.009
Leever, K., Matenco, L., Bertotti, G., Cloetingh, S., & Drijkoningen, K. G. (2006). Late orogenic vertical movements in the Carpathian Bend Zone—Seismic constraints on the transition zone from orogen to foredeep. *Basin Research*, *18*, 521–545. https://doi.org/10.1111/j.1365-2117.2006.00306.x
Liégeois, J.-P., Berza, T., Tatu, M., & Duchesne, J. C. (1996). The Neoproterozoic Pan-African basement from the Alpine Lower Danubian nappe system (South Carpathians, Romania). *Precambrian Research*, *80*(3), 281–301. https://doi.org/10.1016/S0301-9268(96)00019-8

Lobach-Zhuchenko, S. B., Baltybaev, S. K., Glebovitsky, V. A., Sergeev, S. A., Lokhov, K. O., Egorova, Y. S., et al. (2018). U–Pb SHRIMP II age and origin of zircon from lhertzolite of the Bug Paleoarchean complex, Ukrainian Shield. *Doklady Earth Sciences*, *477*(2), 1391–1395. https://doi.org/10.1134/S1028334X17120157

Lowe, D. R. (1982). Sediment gravity flows; II, Depositional models with special reference to the deposits of high-density turbidity currents. *Journal of Sedimentary Research*, *52*(1), 279–297. https://doi.org/10.1306/212F7F31-2B24-11D7-8648000102C1865D

Marshak, S. (1988). Kinematics of orocline and arc formation in thin-skinned orogens. *Tectonics*, *7*, 73–86. https://doi.org/10.1029/tc007i001p00073

Martin, M., & Wenzel, F. (2006). High-resolution teleseismic body wave tomography beneath SE-Romania – II. Imaging of a slab detachment scenario. *Geophysical Journal International*, *164*(3), 579–595. https://doi.org/10.1111/j.1365-246X.2006.02884.x

Mărunțiu, M., Johan, V., Iancu, V., Ledru, P., & Cocherie, A. (1997). Kyanite-bearing eclogite from the Leaota Mountains (South Carpathians, Romania): Mineral associations and metamorphic evolution. *Comptes rendus de l'Académie des Sciences Paris*, *325*, 831–838. https://doi.org/10.1016/S1251-8050(99)80182-7

Mațenco, L. (2017). Tectonics and exhumation of Romanian Carpathians: Inferences from kinematic and thermochronological studies. In M. Radoane, & A. Vespremeanu-Stroe (Eds.), *Landform dynamics and evolution in Romania* (Vol. 1 pp. 15–56). Switzerland: Springer Geography. https://doi.org/10.1007/978-3-319-32589-7_2

Mațenco, L., Bertotti, G., Leever, K., Cloetingh, S., Schmid, S., Tărăpoancă, M., & Dinu, C. (2007). Large-scale deformation in a locked collisional boundary: Interplay between subsidence and uplift, intraplate stress, and inherited lithospheric structure in the late stage of the SE Carpathians evolution. *Tectonics*, *26*, TC4011. https://doi.org/10.1029/2006TC001951

Mațenco, L., Krézsek, C., Merten, S., Schmid, S., Cloetingh, S., & Andriessen, P. (2010). Characteristics of collisional orogens with low topographic build-up: An example from the Carpathians. *Terra Nova*, *22*, 155–165. https://doi.org/10.1111/j.1365-3121.2010.00931.x

Mațenco, L., Munteanu, I., Borgh, M., Stanica, A., Tiliță, M., Lericolais, G., et al. (2016). The interplay between tectonics, sediment dynamics and gateways evolution in the Danube system from the Pannonian Basin to the western Black Sea. *Science of the Total Environment*, *543*, 807–827. https://doi.org/10.1016/j.scitotenv.2015.10.081

Mațenco, L., & Schmid, S. M. (1999). Exhumation of the Danubian nappes system (South Carpathians) during the Early Tertiary: Inferences from kinematic and paleostress analysis at the Getic/Danubian nappes contact. *Tectonophysics*, *314*(4), 401–422. https://doi.org/10.1016/S0040-1951(99)00221-8

Medaris, G., Ducea, M., Ghent, E., & Iancu, V. (2003). Timing of high-pressure metamorphism in the Getic-Supragetic basement nappes of the South-Carpathian mountains fold-thrust belt. *Lithos*, *70*, 141–161. https://doi.org/10.1016/S0024-4937(03)00096-3

Melinte-Dobrinescu, M. C., & Jipa, D. C. (2007). Stratigraphy of the Lower Cretaceous sediments from the Carpathian Bend Area, Romania. *Acta Geologica Sinica*, *81*(6), 949–956. https://doi.org/10.1111/j.1755-6724.2007.tb01018.x

Melinte-Dobrinescu, M. C., & Roban, R. D. (2011). Cretaceous oxic-anoxic changes in the Romanian Carpathians. *Sedimentary Geology*, *235*, 79–90. https://doi.org/10.1016/j.sedgeo.2010.06.009

Melinte-Dobrinescu, M. C., Roban, R. D., & Stoica, M. (2015). Palaeoenvironmental changes across the Albian-Cenomanian boundary interval of the Eastern Carpathians. *Cretaceous Research*, *54*, 68–85. https://doi.org/10.1016/j.cretres.2014.10.010

Menant, A., Jolivet, L., & Vrielynck, B. (2016). Kinematic reconstructions and magmatic evolution illuminating crustal and mantle dynamics of the eastern Mediterranean region since the late Cretaceous. *Tectonophysics*, *675*, 103–140. https://doi.org/10.1016/j.tecto.2016.03.007

Merten, S., Mațenco, L., Foeken, J. P. T., Stuart, F. M., & Andriessen, P. A. M. (2010). From nappe stacking to out-of-sequence postcollisional deformations: Cretaceous to quaternary exhumation history of the SE Carpathians assessed by low-temperature thermochronology. *Tectonics*, *29*, TC3013. https://doi.org/10.1029/2009TC002550

Miall, A. D. (2000). *Principles of sedimentary basin analysis (third, updated and enlarged edition)* (p. 616). Springer-Verlag.

Michalík, M., Budzyń, B., & Gehrels, G. (2006). Cadomian granitoid clasts derived from the Silesian Ridge (results of the study of gneiss pebbles from Gródek at the Jezioro Rożnowskie lake). *Mineralogia Polonica*, *29*, 168–171.

Miclăuş, C., Loiacono, F., Puglisi, D., & Baciu, D. (2009). Eocene-Oligocene sedimentation in the external areas of the Moldavide basin (Marginal Folds Nappe, Eastern Carpathians, Romania): Sedimentological, paleontological and petrographic approaches. *Geologica Carpathica*, *60*, 397–417. https://doi.org/10.2478/v10096-009-0029-9

Mihăilescu, N. G., & Contescu, L. R. (1966). *Sisteme de paleocurenti în flişul curbicortical din Bazinul Văii Bistriţei: o discuţie despre curenţii longitudinali şi transversali* (Vol. LIII(3), pp. 173–194). Bucharest: Dări de seamă ale şedinţelor IGR, Sedimentologie.

Morley, C. K. (1996). Models for relative motion of crustal blocks within the Carpathian region, based on restorations of the outer Carpathian thrust sheets. *Tectonics*, *15*(4), 885–904. https://doi.org/10.1029/95TC03681

Mulder, T., & Alexander, J. (2001). The physical character of subaqueous sedimentary density currents and their deposits. *Sedimentology*, *48*, 269–299. https://doi.org/10.1046/j.1365-3091.2001.00360.x

Murgeanu, G. (1937). *Sur une cordillère antésénonienne dans le géosynclinal du flysch carpatique, Comptes rendus des séances de l'Institut Géologique de Roumanie* (Vol. XXI, pp. 69–85). Bucarest.

Mutti, E., & Ricci-Lucchi, F. (1972). *Le torbiditi dell' Appennino settentrionale: introduzione all'analisi di facies: Memorie della Societa'Geologica Italiana, v. U* (pp. 161–199).

Oaie, G., Seghedi, A., Rădan, S., & Vaida, M. (2005). Sedimentology and source area composition for the Neoproterozoic-Eocambrian turbidites from East Moesia. *Geologica Belgica*, *8/4*, 78–105.

Okay, A. I., & Nikishin, A. M. (2015). Tectonic evolution of the southern margin of Laurasia in the Black Sea region. *International Geology Review*, *57*(5–8), 1051–1076. https://doi.org/10.1080/00206814.2015.1010609

Olariu, C., Jipa, D. C., Steel, R. J., & Melinte-Dobrinescu, M. C. (2014). Genetic significance of an Albian conglomerate clastic wedge, Eastern Carpathians (Romania). *Sedimentary Geology*, *299*, 42–59. https://doi.org/10.1016/j.sedgeo.2013.10.004

Oszczypko, N. (2006). Late Jurassic-Miocene evolution of the Outer Carpathian fold-and-thrust belt and its foredeep basin (Western Carpathians, Poland). *Geological Quaterly*, *50*, 169–194.

Pastor-Galán, D., Gutiérrez-Alonso, G., Murphy, J. B., Fernández-Suárez, J., Hofmann, M., & Linnemann, U. (2013). Provenance analysis of the Paleozoic sequences of the northern Gondwana margin in NW Iberia: Passive margin to Variscan collision and orocline development. *Gondwana Research*, *23*(3), 1089–1103. https://doi.org/10.1016/j.gr.2012.06.015

Patrulius, D. (1969). *Geologia Masivului Bucegi şi a Culoarului Dâmbovicioara* (pp. 321). Bucuresti: Editura Academiei Române.

Pecha, M. E., Gehrels, G. E., Karlstrom, K. E., Dickinson, W. R., Donahue, M. S., Gonzales, D. A., & Blum, M. D. (2018). Provenance of Cretaceous through Eocene strata of the Four Corners region: Insights from detrital zircons in the San Juan Basin, New Mexico and Colorado. *Geosphere*, *14*(2), 785–811. https://doi.org/10.1130/ges01485.1

Pfiffner, O. A. (2006). Thick-skinned and thin-skinned styles of continental contraction. In S. Mazzoli, & R. W. H. Butler (Eds.), *Styles of continental contraction* (pp. 177). Geological Society of America. https://doi.org/10.1130/SPE414

Plašienka, D. (2018). Continuity and episodicity in the early Alpine tectonic evolution of the Western Carpathians: How large-scale processes are expressed by the orogenic architecture and rock record data. *Tectonics*, *37*, 2029–2079. https://doi.org/10.1029/2017TC004779

Posamentier, H. W., & Walker, R. G. (2006). *Facies models revisited* (Vol. 84). Society for Sedimentary Geology. https://doi.org/10.2110/pec.06.84

Postma, G., Kleverlaan, K., & Cartigny, M. J. B. (2014). Recognition of cyclic steps in sandy and gravelly turbidite sequences, and consequences for the Bouma facies model. *Sedimentology*, *61*(7), 2268–2290.

Răbăgia, T., Roban, R. D., & Tarapoanca, M. (2011). Sedimentary records of Paleogene (Eocene to Lowermost Miocene) deformations near the contact between the Carpathian Thrust Belt and Moesia. *Oil & Gas Science and Technology - Revue d'IFP Energies nouvelles*, *66*(6), 931–952. https://doi.org/10.2516/ogst/2011146

Reiser, M. K., Schuster, R., Tropper, P., & Fügenschuh, B. (2017). Constraints on the depositional age and tectono-metamorphic evolution of marbles from the Biharia Nappe System (Apuseni Mountains, Romania). *Geologica Carpathica*, *68*(2), 147–164. https://doi.org/10.1515/geoca-2017-0012

Roban, R., & Melinte-Dobrinescu, M. C. (2012). Lower Cretaceous lithofacies of the Audia Formation Tarcău Nappe, Eastern Carpathians: Genetic significance and palaeoenvironments. *Cretaceous Research*, *38*, 52–67. https://doi.org/10.1016/j.cretres.2012.06.002

Roban, R. D., Krézsek, C., & Melinte-Dobrinescu, M. C. (2017). Cretaceous sedimentation in the outer Eastern Carpathians: Implications for the facies model reconstruction of the Moldavide Basin. *Sedimentary Geology*, *354*, 24–42. https://doi.org/10.1016/j.sedgeo.2017.04.001

Roure, F. (2008). Foreland and Hinterland basins: What controls their evolution? *Swiss Journal of Geosciences*, *101*, 5–29. https://doi.org/10.1007/s00015-008-1285-x

Roure, F., Roca, E., & Sassi, W. (1993). The Neogene evolution of the outer Carpathian flysch units (Poland, Ukraine and Romania): Kinematics of a foreland/fold-and-thrust belt system. *Sedimentary Geology*, *86*, 177–201. https://doi.org/10.1016/0037-0738(93)90139-V

Saintot, A., Stephenson, R. A., Stovba, S., Brunet, M.-F., Yegorova, T., & Starostenko, V. (2006). The evolution of the southern margin of eastern Europe (Eastern European and Scythian platforms) from the Latest Precambrian–Early Palaeozoic to the Early Cretaceous. In D. Gee, & R. A. Stephenson (Eds.), *European Lithosphere Dynamics* (pp. 481–505). London: Geol. Soc., London Mem.

Sanders, C., Andriessen, P., & Cloetingh, S. (1999). Life cycle of the East Carpathian Orogen: Erosion history of a doubly vergent critical wedge assessed by fission track thermochronology. *Journal of Geophysical Research*, *104*, 29,095–29,112. https://doi.org/10.1029/1998JB900046

Săndulescu, M. (1975). Essai de synthese structurale des Carpathes. *Bulletin de la Société géologique de France*, *XVII*, 299. https://doi.org/10.2113/gssgfbull.s7-xvii.3.299

Săndulescu, M. (1984). *Geotectonics of Romania* (p. 336). Bucharest: Editura Tehnică.

Săndulescu, M. (1988). Cenozoic tectonic history of the Carpathians. In L. H. Royden, & F. Horvath (Eds.), *The Pannonian basin, a study in basin evolution* (Vol. 45, pp. 17–25). AAPG Memoir.

Săndulescu, M. (1994). Overview on Romanian geology. 2. Alcapa Congress, Field guidebook. *Romanian Journal of Tectonics and Regional Geology*, *75*(Suppl. 2), 3–15.

Săndulescu, M., Krautner, H. G., Balintoni, I., Russo-Săndulescu, D., & Micu, M. (1981a). The structure of the East Carpathians (Moldavia-Maramureş Area). In *Guidebook Series of the Geological Institute of Romania* (Vol. 21, p. 91).

Săndulescu, M., Ştefănescu, M., Butac, A., Pătruţ, I., & Zaharescu, P. (1981b). Genetical and structural relations between Flysch and Molasse (the East Carpathians Model). In *Guidebook Series of the Geological Institute of Romania* (Vol. 19, p. 94).

Săndulescu, M., & Visarion, M. (1978). *Considérations sur la structure tectonique du soubassement de la Dépression de Transylvanie. Dari de seama ale sedintelor IGR* (Vol. LXIV/5, pp. 153–173). Bucharest.

Săndulescu, M., & Visarion, M. (1988). La structure des plateformes situées dans l'avant-pays et au-dessous des nappes du flysch des Carpathes orientales, Studii tehnice şi economice. *Geofizică*, *15*, 62–67.

Schmid, S. M., Bernoulli, D., Fügenschuh, B., Georgiev, N., Kounov, A., Maţenco, L., et al. (2020). Tectonic units of the Alpine collision zone between Eastern Alps and Western Turkey. *Gondwana Research*, *78*, 308–374. https://doi.org/10.1016/j.gr.2019.07.005

Schmid, S. M., Bernoulli, D., Fügenschuh, B., Maţenco, L., Schefer, S., Schuster, R., et al. (2008). The Alpine-Carpathian-Dinaridic orogenic system: Correlation and evolution of tectonic units. *Swiss Journal of Geosciences*, *101*(1), 139–183. https://doi.org/10.1007/s00015-008-1247-3

Schmid, S. M., Berza, T., Diaconescu, V., Froitzheim, N., & Fügenschuh, B. (1998). Orogen-parallel extension in the Southern Carpathians. *Tectonophysics*, *297*, 209–228. https://doi.org/10.1016/S0040-1951(98)00169-3

Seghedi, A. (2001). The North Dobrogea orogenic belt (Romania): A review. In P. A. Ziegler, W. Cavazza, & A. F. H. Robertson (Eds.), *Peri-Tethys memoir 6: Peri-Tethyan rift/wrench basins and passive margins* (Vol. 186, pp. 237–257). Memoir du Muséum d'histoire naturelle.

Seghedi, A., Berza, T., Iancu, V., Mărunţiu, M., & Oaie, G. (2005). Neoproterozoic terranes in the Moesian basement and in the Alpine Danubian nappes of the South Carpathians. *Geologica Belgica*, *8*(4), 4–19.

Seghedi, A., Oaie, G., Iordan, M., Avram, E., Tatu, M., Ciulavu, D., et al. (1999). Excursion guide of the joint meeting of EUROPROBE TESZ, PANCARDI and GEORIFT projects: "Dobrogea– the interface between the Carpathians and the Trans-European Suture Zone": Geology and structure of the Precambrian and Paleozoic basement of North and Central Dobrogea. Mesozoic history of North and Central Dobrogea. *Romanian Journal of Tectonics and Regional Geology*, *77*.

Seghedi, A., Oaie, G., Vaida, M., Debacker, T. N., & Sintubin, M. (2004). *Paleozoic formations in North Dobrogea: Sedimentation deformation and metamorphism, Avalonia-Moesia Symposium and Workshop* (pp. 31–32). Ghent/Ronse, Belgium.

Shumlyanskyy, L., Billstrom, K., Hawkesworth, C., & Elming, S.-A. (2012). U-Pb age and Hf isotope compositions of zircons from the north-western region of the Ukrainian shield: mantle melting in response to post-collision extension. *Terra Nova*, *24*, 373–379. https://doi.org/10.1111/j.1365-3121.2012.01075.x

Shumlyanskyy, L., Hawkesworth, C., Dhuime, B., Billstrom, K., Claesson, S., & Storey, C. (2015). $^{207}Pb/^{206}Pb$ ages and Hf isotope composition of zircons from sedimentary rocks of the Ukrainian shield: Crustal growth of the south-western part of East European craton from Archaean to Neoproterozoic. *Precambrian Research*, *260*, 39–54. https://doi.org/10.1016/j.precamres.2015.01.007

Sprague, A. R. G., Garfield, T. R., Goulding, F. J., Beauboef, R. T., Sullivan, M. D., Rossen, C., et al. (2005). *Integrated slope channel depositional models: The key to successful prediction of reservoir presence and quality in offshore West Africa. E-Exitep* (pp. 1–13). Veracruz, Mexico: Colegio de Ingenenieros Petroleros de Mexico.

Stampfli, G. M., & Borel, G. D. (2002). A plate tectonic model for the Paleozoic and Mesozoic constrained by dynamic plate boundaries and restored synthetic oceanic isochrones. *Earth and Planetary Science Letters*, *196*, 17–33. https://doi.org/10.1016/S0012-821X(01)00588-X

Ştefănescu, M. (1976). *O nouă imagine a structurii flişului intern din regiunea de curbură a Carpaţilor* (Vol. LXII(5), pp. 257–259). Bucuresti: Dări de Seamă ale Sedinţelor - Institutul de Geologie şi Geofizică.
Ştefănescu, M. (1983). General remarks on the Eastern Carpathians flysch and its depositional environment. *Revue roumaine de géologie, géophysique et géographie*, *27*, 59–64.
Stoica, A. M., Ducea, M. N., Roban, R. D., & Jianu, D. (2016). Origin and evolution of the South Carpathians basement (Romania): A zircon and monazite geochronologic study of its Alpine sedimentary cover. *International Geology Review*, *58*(4), 510–524. https://doi.org/10.1080/00206814.2015.1092097
Strachan, L. J., Rarity, F., Gawthorpe, R. L., Wilson, P., Sharp, I., & Hodgetts, D. (2013). Submarine slope processes in rift-margin basins, Miocene Suez Rift, Egypt. *GSA Bulletin*, *125*(1-2), 109–127. https://doi.org/10.1130/b30665.1
Štrba, L. (2012). Deep-marine channel deposits of Cotumba-Sita-T_x001CE;taru Sandstones, Teleajen Valley, Romania (East Carpathian Flysch Zone). *Studia UBB Geologia*, *57*(2), 27–34. https://doi.org/10.5038/1937-8602.57.2.3
Świdrowska, J., Hakenberg, M., Poluhtovič, B., Seghedi, A., & Višnâkov, I. (2008). Evolution of the Mesozoic basins on the southwestern edge of the East European Craton (Poland, Ukraine, Moldova, Romania). *Studia Geologica Polonica*, *130*, 3–130.
Tari, G. (2005). *The divergent continental margins of the Jurassic proto Pannonian Basin: implications for the petroleum systems of the Vienna Basin and the Moesian Platform. Transactions GCSSEPM Foundation 25th Annual Research Conference* (pp. 955–986). Viena.
Tari, G., Dicea, O., Faulkerson, J., Georgiev, G., Popov, S., Stefanescu, M., & Weir, G. (1997). Cimmerian and Alpine stratigraphy and structural evolution of the Moesian Platform (Romania/Bulgaria). In A. G. Robinson (Ed.), *Regional and petroleum geology of the Black Sea and surrounding region* (Vol. 68, pp. 63–90). AAPG Memoir.
Tikhomirov, P., Chalot-Prat, F., & Nazarevich, B. P. (2004). Triassic volcanism in the Eastern Fore-Caucasus: Evolution and geodynamic interpretation. *Tectonophysics*, *381*(1-4), 119–142. https://doi.org/10.1016/j.tecto.2003.10.014
Torsvik, T. H., Steinberger, B., Gurnis, M., & Gaina, C. (2010). Plate tectonics and net lithosphere rotation over the past 150 My. *Earth and Planetary Science Letters*, *291*(1), 106–112. https://doi.org/10.1016/j.epsl.2009.12.055
Tucker, E. M. (2011). *Sedimentary rocks in the field: A practical guide* (4th ed.p. 275). Wiley-Blackwell.
Ustaszewski, K., Schmid, S. M., Fügenschuh, B., Tischler, M., Kissling, E., & Spakman, W. (2008). A map-view restoration of the Alpine-Carpathian-Dinaridic system for the Early Miocene. *Swiss Journal of Geosciences*, *101*(1), 273–294. https://doi.org/10.1007/s00015-008-1288-7
Vaida, M., Seghedi, A., & Verniers, J. (2005). Northern Gondwanan affinity of the East Moesian Terrane based on chitinozoans. *Tectonophysics*, *410*, 379–387. https://doi.org/10.1016/j.tecto.2004.12.039
van Hinsbergen, D., Torsvik, J. J., Schmid, T. H., Maţenco, S. M. L. C., Maffione, M., Vissers, R. L. M., et al. (2020). Kinematic reconstruction and tectonic evolution of the Mediterranean region since the Triassic. *Gondwana Research*, *81*, 79–229. https://doi.org/10.1016/j.gr.2019.07.009
Visarion, M., Săndulescu, M., Stănică, D., & Veliciu, S. (1988). Contributions á la connaissance de la structure profonde de la plateforme Moésienne en Roumanie, Studii tehnice şi economice. *Geofizică*, *15*, 68–92.
von Raumer, J. F., Bussy, F., Schaltegger, U., Schulz, B., & Stampfli, G. M. (2013). Pre-Mesozoic Alpine basements—their place in the European Paleozoic framework. *Geological Society of America Bulletin*, *125*, 89–108. https://doi.org/10.1130/B30654.1
Walker, R. G. (1992). Facies, facies models and modern satigraphic concepts. In R. G. Walker, & N. P. James (Eds.), *Facies models response to sea level change* (pp. 1–15). Canada: Geological Association of Canada.
Zelazniewicz, A., Bula, Z., Ning, M. F., Seghedi, A., & Zaba, J. (2009). More evidence on Neoproterozoic terranes in Southern Poland and south-eastern Romania. *Geological Quarterly*, *53*(1), 93–124.

References From the Supporting Information

Alexandrescu, G. (1971). *Studiul flişului intern şi extern dintre valea Bistricioarei şi valea Moldovei (Carpaţii Orientali), Unpublished PhD Thesis* (p. 240). Bucuresti: [in Romanian, with French abstract].
Grasu, C., Catană, C., & Boboş, L. (1996). *Petrografia formaţiunilor din flişul intern carpatic*. Editura Tehnică Bucureşti. 178 pp
Grasu, C., Catană, C., & Grinea, D. (1988). In *Flişul carpatic. Petrografie şi consideraţii economice* (p. 208 pp). Editura Tehnică. Bucureşti.
Grigorescu, D. (1971). *Studiul stratigrafic al fomaţiunilor "Şisturilor negre" (senso stricto) în perimetrul Valea Covasna-Valea Zăbrătău ("Unitatea Şisturilor Negre") prin metoda microfacială. Unpublished PhD Thesis*. Bucuresti: Bucharest University. [in Romanian, with English abstract]
Hailwood, E., & Ding, F. (2000). Sediment transport and dispersal pathways in the Lower Cretaceous sands of the Britannia Field, derived from magnetic anisotropy. *Petroleum Geoscience*, *6*, 369–379. https://doi.org/10.1144/petgeo.6.4.369
Hrouda, F. (1982). Magnetic anisotropy of rocks and its application in geology and geophysics. *Geophysical Surveys*, *5*(1), 37–82. https://doi.org/10.1007/BF01450244
Hu, X., Jansa, L., Wang, C., Sarti, M., Bąk, K., Wagreich, M., et al. (2005). Upper Cretaceous oceanic red beds (CORBs) in the Tethys: Occurrences, lithofacies, age, and environments. *Cretaceous Research*, *26*, 3–20. https://doi.org/10.1016/j.cretres.2004.11.011
Hu, X., Scott, R., Cai, Y., Wang, C., & Melinte-Dobrinescu, M. C. (2012). Cretaceous Oceanic Red Beds (CORBs): Different time scales, different origin models. *Earth Science Reviews*, *115*, 217–248. https://doi.org/10.1016/j.earscirev.2012.09.007
Jelinek, V. (1977). The statistical theory of measuring anisotropy of magnetic susceptibility of rocks and its application. *Geofyzika Brno*, *88*.
Jelinek, V. (1981). Characterization of the magnetic fabric of rocks. *Tectonophysics*, *79*, T63–T67. https://doi.org/10.1016/0040-1951(81)90110-4
Liu, B., Saito, Y., Yamazaki, T., Abdeldayem, A., Oda, H., Hori, K., & Zhao, Q. (2001). Paleocurrent analysis for the Late Pleistocene-Holocene incised-valley fill of the Yangtze delta, China by using anisotropy of magnetic susceptibility data. *Marine Geology*, *176*(1-4), 175–189. https://doi.org/10.1016/S0025-3227(01)00151-7
Maffione, M., Hernandez-Moreno, C., Ghiglione, M. C., Speranza, F., van Hinsbergen, D. J. J., & Lodolo, E. (2015). Constraints on deformation of the Southern Andes since the Cretaceous from anisotropy of magnetic susceptibility. *Tectonophysics*, *665*, 236–250. https://doi.org/10.1016/j.tecto.2015.10.008
Melinte-Dobrinescu, M. C., Brustur, T., Jipa, D., & Szobotka, S. A. (2009). Eastern Carpathian Cretaceous oceanic red beds: Lithofacies, biostratigraphy and paleoenvironment. In X. Hu, C. Wang, R. W. Scott, M. Wagreich, & L. Jansa (Eds.), *Cretaceous oceanic red beds: Stratigraphy, composition, origins and paleoceanographic/paleoclimatic significance* (Vol. 91, pp. 91–107). SEPM Special Publication.
Melinte-Dobrinescu, M. C., Roban, R. D., & Stoica, M. (2015). Palaeoenvironmental changes across the Albian-Cenomanian boundary interval of the Eastern Carpathians. *Cretaceous Research*, *54*, 68–85. https://doi.org/10.1016/j.cretres.2014.10.010

Roban, R. D., Krézsek, C., & Melinte-Dobrinescu, M. C. (2017). Cretaceous sedimentation in the outer Eastern Carpathians: Implications for the facies model reconstruction of the Moldavide Basin. *Sedimentary Geology*, *354*, 24–42. https://doi.org/10.1016/j.sedgeo.2017.04.001

Sagnotti, L. (2011). Magnetic anisotropy. In H. K. Gupta (Ed.), *Encyclopedia of solid earth geophysics* (pp. 717–729). Springer Science +Business Media. https://doi.org/10.1007/978-90-481-8702-7_113

Săndulescu, M., Ştefănescu, M., Butac, A., Pătruţ, I., & Zaharescu, P. (1981). Genetical and structural relations between Flysch and Molasse (the East Carpathians Model). In *Guidebook Series of the Geological Institute of Romania* (Vol. 19, pp. 3–94). Bucharest.

Tauxe, L. (2005). *Lectures in paleomagnetism*. http://earthref.org/MAGIC/books/Tauxe/2005/